

**ELECTRONS IN NONPOLAR LIQUIDS**

**Richard A. Holroyd**

Department of Chemistry, Brookhaven National Laboratory, Upton, NY 11973

Table of Contents	Page
I. Introduction	3
II. Electron Escape and Recombination	4
A. $G_{fi}$ for Minimum Ionizing Radiation	6
B. $G_{fi}$ for X-rays	7
C. $G_{fi}$ for Alpha Particles	8
III. Energy of the Quasi-free Electron – $V_0$	9
IV. Solvated Electrons	13
V. Reactions of Electrons	16
A. Electron Equilibria	17
B. Attachment Rate Constants	20
VI. Transport Properties	28
A. Quasi-free mobility	28
B. Trapped State Transport	31
C. Hall Mobility	34
D. Diffusion Coefficient	35
E. Effective Mass	35
F. Fast Negative Ions	35
G. Positron Mobility	36
VII. Applications	37

## Introduction

Excess electrons can be introduced into liquids by absorption of high energy radiation, by photoionization, or by photoinjection from metal surfaces. The electron's chemical and physical properties can then be measured, but this requires that the electrons remain free. That is, the liquid must be sufficiently free of electron attaching impurities for these studies. The drift mobility as well as other transport properties of the electron are discussed here as well as electron reactions, free-ion yields and energy levels.

Ionization processes typically produce electrons with excess kinetic energy. In liquids during thermalization, where this excess energy is lost to bath molecules, the electrons travel some distance from their geminate positive ions. In general the electrons at this point are still within the coulombic field of their geminate ions and a large fraction of the electrons recombine. However, some electrons escape recombination and the yield that escapes to become free electrons and ions is termed  $G_{fi}$ . Reported values of  $G_{fi}$  for molecular liquids range from 0.05 to 1.1 per 100 eV of energy absorbed.[1,2] The reasons for this 20-fold range of yields are discussed here.

Electrons in nonpolar liquids are either in the conduction band, trapped in a cavity in the liquid, or in special cases form solvent anions. The energy of the bottom of the conduction band is termed  $V_0$ .  $V_0$  has been measured for many liquids and its dependence on temperature and pressure has also been measured. New techniques have provided quite accurate values of  $V_0$  for the liquid rare gases. The energies of the trapped state have also been derived for several liquids from studies of equilibrium electron reactions. A characteristic of the trapped electron is its broad absorption spectrum in the infrared.

Electron attachment rates have been measured for numerous solutes. Many of these studies were limited to three solvents: cyclohexane, 2,2,4-trimethylpentane and

tetramethylsilane (TMS) and those rates are discussed here. What to expect in other liquids can be inferred from these results. Considerable insight has been gained into certain reactions. Equilibrium reactions of electrons are particularly interesting since they provide information not only on energy levels, as mentioned above, but also on the partial molar volume of trapped electrons. This has led to a better understanding of the mechanism of electron transport.

This chapter presents the current understanding of electrons in nonpolar liquids. Experimental as well as theoretical studies are discussed. For further detail than is provided here the reader is referred to recent books on the subject,[3,4] as well as references cited herein. Some questions still remain due largely to the theoretical difficulties of describing a quantum particle in a disordered environment. The future will hopefully bring new discoveries and revelations that will answer these questions. Finally, we discuss current applications of nonpolar liquids to indicate where future uses may develop.

## **II. Electron Escape and Recombination**

An important consideration in understanding a radiation chemical mechanism or predicting the outcome of a radiation experiment is knowing the yield of free electrons or  $G_{fi}$ , the number of ion pairs produced per 100 eV absorbed. The free ion yield is affected by the density of ionization along the track of the ionizing particle. The highest yield is observed for high energy electrons, typically 1-2 MeV, which result in well separated clusters of a few ionizations each. An alpha particle creates a dense column of ionization and ion yields are very low. X-rays show intermediate behavior. Other factors like molecular structure, temperature, the applied field, the pressure and density also affect  $G_{fi}$ .

Making sense of free ion yield data requires first knowing what is meant by the free ion yield. Free electrons are those that escape initial spur or track recombination and

are therefore diffusing in the bulk and can react with other species in a homogeneous fashion. The escape process can be considered to have two steps. First, the electrons released by ionizing the solvent molecules lose energy in scattering events and in the process travel some distance,  $r$ , from their positive ions. The electrons may lose energy to vibrational modes but a significant fraction of the range occurs while the electron has lower, near thermal energy. In general there will be a distribution of ranges  $D(r)$  and the mean thermalization range is designated by  $b$ . For most nonpolar liquids the electrons after thermalization will still be within the Coulombic field of the positive ions, equal to  $e^2/\epsilon r$ , where  $\epsilon$  is the dielectric constant. Consequently, the fraction escaping is low.

In the second step the thermalized electrons will either recombine with the ions in the track or spur or escape. The yield of free electrons is the integral of the product  $D(r) \times P(r)$  times the number of electron-ion pairs formed initially in the spur or track,  $G_{\text{tot}}$ , where  $P(r)$  is the probability of escape. For a single ion pair  $P(r)$  is given by:[5]

$$P(r) = \exp(-e^2/\epsilon k_B T) \quad (1)$$

The initial yield,  $G_{\text{tot}}$ , is not known exactly for molecular liquids. However the fraction of electrons that escape geminate recombination increases with the applied electric field and extrapolating such results to high field gives  $G_{\text{tot}} = 4.0$  for neopentane,[6]  $3.1 \pm 0.3$  for TMS,[7] and 4.5 for Ar.[8] A value for  $G_{\text{tot}}$  of 4.0 was obtained for cyclohexane by measuring the yields of methyl radicals formed in the reaction of electrons with methyl chloride and methyl bromide.[9] High concentrations of these solutes were used (up to 0.5 M) in order to compete with geminate recombination. An analysis by Jay-Gerin et al. of free ion yield data led to an average  $G_{\text{tot}}$  value of  $3.7 \pm 0.5$  for typical hydrocarbons. [10] Others have suggested that  $G_{\text{tot}}$  may vary considerably from liquid to liquid.[11]

Fast pulse radiolysis studies have shown that geminate recombination occurs on the picosecond time scale.[12,13] Bartczak and Hummel[14] predicted that for n-dodecane 82% of the geminate ions still remain at 5 ps for 1 MeV irradiation. Future accelerators, with pulses of a few picoseconds length, may soon provide experimental measurements of  $G_{\text{tot}}$  directly.

*A.  $G_{\text{fi}}$  for Minimum Ionizing Radiation.* For minimum ionizing radiation, where the ionization events are widely separated, the value of  $G_{\text{fi}}$  at room temperature correlates with the electron mobility,  $\mu_{\text{D}}$ . [1,10]

Figure 8.1

Figure 8.1 illustrates this dependence for representative liquids. Typically,  $G_{\text{fi}}$  and  $\mu_{\text{D}}$  are low for n-alkanes, n-alkenes and aromatics and high for branched compounds with many methyl groups like neopentane. For  $\mu_{\text{D}} > 0.1 \text{ cm}^2/\text{Vs}$  the yields for alkanes follow reasonably well a relationship suggested by Jay-Gerin:[10]

$$G_{\text{fi}} = a (\mu_{\text{D}})^x \quad (2)$$

Implicit in such a dependence is the recognition that scattering lengths of thermal and epithermal electrons are similar. A least squares fit of the data for compounds containing only hydrogen and carbon leads to the solid line shown in figure 8.1 for which  $a = 0.25$  and  $x = 0.33$ , for  $\mu_{\text{D}}$  in  $\text{cm}^2/\text{Vs}$ .

Figure 8.1 includes points for ethane and propane at 298 K for which  $G_{\text{fi}} = 0.94$  and 0.43 ions/100 eV, respectively.[16] The electron mobilities for these liquids at this temperature are quite high. At even higher temperatures, in the supercritical fluid,  $G_{\text{fi}}$  and  $\mu_{\text{D}}$  for ethane and propane are higher still.[20,21] On the other hand, at low temperatures near the boiling points the yields of free ions as well as the mobilities in these liquids are quite low ( $G_{\text{fi}} = 0.16$  for ethane for example) and points for these liquids then would be on the left side of the figure.

The data for compounds containing a silicon or germanium atom fall on a lower line (dashed) in figure 8.1 for which  $a = 0.12$  and  $x = 0.34$  in Eq. 2. That is, for any given mobility value, compounds containing a heavier atom have a lower free ion yield than that given by the line for alkanes.[15] A lower  $G_{fi}$  means a shorter mean thermalization range, suggesting that scattering of epithermal electrons is stronger when silicon or germanium atoms are present. The points for benzene and toluene are also below the line for alkanes. While Eq. 2 is a rough prediction of how  $G_{fi}$  changes with mobility it fails in some cases. For example, when pressure is applied to 2,2-dimethylbutane and 2,2,4-trimethylpentane  $\mu_D$  increases yet  $G_{fi}$  decreases.[22] However, for *n*-pentane and TMS Eq. 2 predicts the changes in  $G_{fi}$  with pressure quite well.

Free ion yields generally increase with increasing temperature, indicating that the mean thermalization distance,  $b$ , increases. Since the density,  $d$ , decreases with increasing temperature, several authors have examined how the product,  $bd$ , changes. In the case of *n*-alkanes and benzene this product is fairly constant over a large temperature range.[17] This same study also found that at 296 K  $bd$  is almost the same for the alkanes from  $C_4$  to  $C_{14}$ . For the pressure study mentioned above, free ion yields were found to decrease with increasing pressure yet the product,  $bd$ , remained quite constant for all six liquids studied.[22]

*B.  $G_{fi}$  for X-rays.* Yields of free ions for exposure to x-rays are less than for high energy electrons. Interaction of x-rays with nonpolar liquids occurs largely by the photoelectric effect, with Compton scattering becoming important as the photon energy increases. Both events release electrons. The photoelectron energy is given by the x-ray energy less the binding energy, which for carbon is 284 eV. For hydrocarbons, photoelectrons from the k-shell of carbon will dominate.

Figure 8.2

Results for x-rays are shown in figure 8.2.  $G_{fi}$  has been measured for three liquids for x-rays of 1.6 to 30 keV energy.[23-25] The figure also includes points for minimum ionizing radiation at 2 MeV. There are very large changes in yield with energy. For 2,2,4,4-tetramethylpentane  $G_{fi}$  changes from 0.83 to 0.12 ions/100 eV. The probability of escape is only 3% in the 2-5 keV range.

The lower yields for x-rays come about as a result of the high rate of energy loss of the photoelectrons resulting in a high density of ionizations along the track of the electron. This rate of energy loss depends on the energy of the photoelectrons. For a 30 keV electron, ionizations occur on average 24 nm apart, while for a 2 keV electron ionizations occur 2.9 nm apart. Thus there is overlap of ionizations because the thermalization ranges of the secondary electrons are comparable to the distance between ionizations. A secondary electron will sense several positive ions along the track, thus increasing the probability of recombination in the track.

Theoretical calculations of the free ion yields have been made as a function of the electron energy. These calculations start with a given track structure for the position of the positive ions and a distribution of distances for the secondary electrons. The charges are then allowed to diffuse in the electric field due to all the other charges. Electrons either recombine with positive ions or escape. The lines in figure 8.2 were calculated in this way. The dashed lines are for n-hexane and 2,2,4-trimethylpentane. In this case a Gaussian distribution of electron separation distances was assumed, with the mean thermalization ranges,  $b$ , shown on the figure.[26,29] For the dotted line an exponential distribution with an average thermalization range of 26.5 nm was assumed.[27] The computer simulations agree quite well with the experimental measurements.

*C.  $G_{fi}$  for alpha particles.* The few studies that have been made indicate that the free ion yield for exposure of liquids to alpha particles is quite small. For hydrocarbons

$G_{fi}$  is very small, 0.005 per 100 eV.[30,31] Theoretically a zero yield is expected for cylindrical geometry and alpha particles create such a track. The low yields in hydrocarbons can be attributed to those electrons on the tail of the distribution that thermalize some distance from the track, these are often called delta rays. For liquid rare gases the yields are higher, for example the zero field yield is 0.16 per 100 eV for Xe,[32] because the thermalization ranges are much longer.

### **III. Energy of the Quasi-free Electron.**

The existence of a band of states in which the electron is quite mobile and its wave-function is extended is common to all nonpolar liquids. The energy of the lowest state in this band relative to vacuum is designated  $V_0$ . Values of  $V_0$  for nonpolar molecular liquids range from +0.2 to -0.75 eV at room temperature.[2] Some representative values are given in Table 8.1. When  $V_0$  is low in energy there is usually

Table 8.1

little trapping and the electron mobility is high. Conversely when  $V_0$  is high, the trap state is likely to be favored and the mobility is low. When  $V_0$  is positive the electron favors the vacuum over the liquid, energetically. Emission of electrons into the vacuum occurs readily for liquids for which  $V_0$  is positive like n-hexane ( $V_0 = 0.1$  eV)[35,36]. For liquid helium  $V_0$  is +1.3 eV and the electron resides in a bubble of radius 1.4 nm.[37]

The energy of the  $V_0$  state is usually considered to be the difference between two terms: an attractive polarization energy,  $U_p$ , and a kinetic energy term,  $T_0$ . Conceptually, this energy is like the energy of the ground state of an electron in a potential well, where the walls of the well are the impenetrable hard sphere surfaces of the molecules of the fluid. When these walls come closer, the energy  $T_0$  will increase, which explains why  $V_0$  increases with density for liquids. For example,  $V_0$  increases with decreasing temperature for various hydrocarbons.[38] When pressures of 2.5 kbar are applied to hydrocarbons,

increases in  $V_0$  of a few tenths of an eV are observed. [39] Various theories have been used to calculate  $V_0$ , see below.

Several methods have been employed to measure the energy of this state in nonpolar liquids. The methods fall into three categories: the change in work function of a metal when immersed in the liquid; photoionization; and field ionization. Of these the latter, in which field ionization of high-lying Rydberg states is utilized to locate  $V_0$ , has in recent years provided what are considered to be the most accurate values of  $V_0$  in fluid Ar, Kr and Xe.

In the photoelectric method  $V_0$  is obtained as the change in work function,  $\phi$ , of a metal when immersed in the liquid. Thus  $V_0$  is given by the difference in work functions:

$$V_0 = \phi_{\text{liq}} - \phi_{\text{vac}} \quad (3)$$

This method was first used to determine  $V_0$  in liquid Ar, [40] and was later applied to liquid hydrocarbons [38,41-43] as well as to supercritical hydrocarbons like ethane. [44-46] Most of the data available on  $V_0$  for nonpolar liquids was obtained by this method.

In a variation of the photoelectric method,  $V_0$  can be determined by measuring emission of electrons from the liquid into the vacuum. Even when  $V_0$  is negative electrons can penetrate this barrier and be collected in the gas phase. [35,36,47] Borghesani, et al.[48] used this technique and from the time evolution of the current reaching the anode for a sample of liquid Ar at 87 K found  $V_0$  to be  $-0.126$  eV. This is in excellent agreement with the value of  $-0.125$  eV given by equation 6 (see below) for this density ( $2.09 \times 10^{22}$   $\text{cm}^{-3}$ ) using the field ionization technique.

When molecules are photoionized in a liquid there is a lowering of the ionization threshold,  $E_{\text{th}}$ , due to both the sudden polarization of the liquid by the ion  $E_{\text{pol}}^+$  and  $V_0$ . Thus:

$$E_{\text{th}} = IP + E_{\text{pol}}^+ + V_0 \quad (4)$$

A study of the photoionization of TMPD in solution [49] showed the dependence of the wavelength of ionization onset on the energy  $V_0$  of the solvent. The data was used to evaluate  $V_0$  for 18 different liquids. Typical results of this and other studies [50,51] are given in Table 8.1. Direct single-photon ionization of solvent molecules is also sensitive to the value of  $V_0$  [52-55] and can in principle be used to determine  $V_0$ .

Recently, laser multiphoton ionization of solutes has been used. Defining the threshold of ionization,  $E_{th}$ , can be a problem in some of these methods. A recent multiphoton technique, utilizing femtosecond laser pulses, appears to give quite accurate thresholds. [56] In this work a conductivity spectrum is measured at visible wavelengths and a sharp drop in current occurs as the mechanism changes from  $n$ -photon excitation to  $(n+1)$ -photon excitation, where  $n$  is typically 3 to 4. The threshold is defined by fitting the current to an analytic function that defines the midpoint of this transition.  $E_{th}$  is then  $n$  times the energy at which the midpoint occurs. The thresholds are sensitive to  $V_0$  and could be used for determination of this quantity.

Photodetachment from anions should also be mentioned. [57-59] In this case the threshold,  $E_{th}'$ , given by:

$$E_{th}' = E.A. + V_0 - E_{pol}, \quad (5)$$

is well defined since the electron escapes with high probability from the neutral molecule left behind, and the photodetachment yields as a function of photon energy follow a known power law. Thus  $V_0$  values can be determined from such studies if values of the electron affinity, E.A., are available.

Recently  $V_0$  has been measured in dense rare gas fluids by field ionization of Rydberg states of solutes lying close to the continuum. In this technique Reininger and coworkers [60-63] utilized synchrotron radiation and measured photocurrent spectra in the

VUV with a resolution of 7 meV. The photocurrent spectra were measured at several applied electric fields. A field ionization spectrum was obtained by subtracting the spectrum at low field from one obtained at high field. Such spectra typically showed one peak at threshold energies due to those high-lying states that ionized at the high voltage but not at the low. Measurements were made in argon containing CH<sub>3</sub>I [60] and H<sub>2</sub>S [61] as solutes and the density was varied from dilute gas to the triple point of argon. The position of the field ionization peak shifts as the density is changed. These shifts are the combined effect of changes in the ion-media polarization energy and  $V_0$ . Accurate calculation of the former allowed evaluation of  $V_0$  as a function of density, utilizing Eq. 4 above. The resulting values of  $V_0$  are in good agreement with earlier photoelectric and theoretical values. Further, the two solutes: CH<sub>3</sub>I and H<sub>2</sub>S gave very comparable results. For argon,  $V_0$  reaches a minimum value of -0.294 eV at a density of  $12 \times 10^{21} \text{ cm}^{-3}$ , which is the density at which the electron mobility is a maximum.

Figure 8.3

The solid line in Fig. 8.3 is a best fit of Eq. 6 to the experimental data.[61] See cited reference for values of the parameters in equation 6.

$$V_0(N) = a_0 + a_1(N-a_2) + (a_3/a_4) \ln \cosh(a_4(N-a_2)) \quad (6)$$

The density dependence of  $V_0$  in Kr was determined by field ionization of CH<sub>3</sub>I [62] and (CH<sub>3</sub>)<sub>2</sub>S [63]. Whereas previous studies found a minimum in  $V_0$  at a density of  $12 \times 10^{21} \text{ cm}^{-3}$ , [66] the new study indicates the minimum is at  $14.4 \times 10^{21} \text{ cm}^{-3}$  (see Fig 8.3). This is very close to the density of  $14.1 \times 10^{21} \text{ cm}^{-3}$  at which the electron mobility reaches a maximum in krypton, [67] a result that is consistent with the deformation potential model [68] which predicts the mobility maximum to occur at a density where  $V_0$  is a minimum. The use of (CH<sub>3</sub>)<sub>2</sub>S permitted similar measurements of  $V_0$  in Xe because of its lower ionization potential. The results for Xe are also shown in Fig 8.3 by the lower

line, which represents the analytical equation 6 giving the best fit to the data. Parameter values,  $a_n$ , can be found in the reference cited.

The earliest theoretical model of the effect of a medium on the quasi-free electron energy was proposed by Fermi [69] to explain ionization of high Rydberg states. This model, which predicts a linear dependence on density, works well only at low densities. Springett, Jortner and Cohen [37] introduced the Wigner-Seitz model to calculate  $V_0$  in several liquids employing a simple electron-atom pseudopotential. This model was used by Stampfli and Bennemann to calculate  $V_0$  for liquid Ar, Kr, and Xe, except they solved the eigenvalue problem numerically.[64] Their results for Ar, shown in Fig. 8.3 by the dashed line, are in good agreement with experiment. Several other modifications to the theoretical treatments have been proposed [65,70-73] using various techniques. Simon, et al. used a classical percolation approach to predict  $V_0$  for Ar, Kr, and Xe.[74,75] The calculations of Plenkiewicz, et al., [65] which use an accurate electron-atom pseudopotential, are shown by the dotted lines in Fig 8.3. Their calculations also agree quite well with the experimental data and find the minima at the right densities. These newer studies are readily applicable to molecular liquids and have been applied to  $\text{CH}_4$  and  $\text{SiH}_4$ . [76]

#### **IV. Solvated Electrons**

Evidence for the existence of a trapped state of the electron in some liquids comes from several sources. For one, pulse radiolysis studies have shown that for certain alkanes there is a broad absorption in the infrared that can be attributed to the electron. Second, studies of the effect of pressure on the mobility of electrons have revealed information about cavity sizes and the role of electrostriction in the trapping process. Finally, conductivity studies of reversible reactions of the electron have given us the energetics of the trapping process. These latter equilibrium studies are described in detail in section V-A. Values of  $\Delta G_{\text{soln}}(e)$  for selected liquids

are given in Table 8.1. For many liquids  $\Delta G_{\text{soln}}(e)$  lies below the  $V_0$  state making trapping energetically favorable.

Early pulse radiolysis studies of alkanes at room temperature showed that the solvated electron absorption begins around 1  $\mu\text{m}$  and increases with increasing wavelength to 1.6  $\mu\text{m}$  for n-hexane, cyclohexane and 2-methylbutane.[77] More complete spectra for three liquid alkanes are shown in Figure 8.4. The spectrum for methylcyclohexane at 295 K

Figure 8.4

extends to 4  $\mu\text{m}$  and shows a peak at 3.25  $\mu\text{m}$ . [78] At the maximum the extinction coefficient is  $2.8 \times 10^4 \text{ M}^{-1}\text{cm}^{-1}$ . The spectrum for 3-methyloctane at 127 K, shown in Figure 8.4, peaks around 2  $\mu\text{m}$ . The peak for methylcyclohexane is also at 2  $\mu\text{m}$  at lower temperatures. Recently, the absorption spectra of solvated electrons in 2-methylpentane, 3-methylpentane, cis-decalin and methylcyclohexane glasses have been measured accurately at 77 K.[80] For these alkanes the maxima occur at 1.8  $\mu\text{m}$ , where the extinction coefficient is  $2.7 \times 10^4 \text{ M}^{-1}\text{cm}^{-1}$ .

The stronger absorption at lower temperatures can be attributed to several factors. One is that the equilibrium between quasifree and trapped electrons shifts to favor trapped electrons as the temperature is lowered for these liquids. Another is that homogeneous recombination of electrons with positive ions is slower at the lower temperatures and therefore occurs to a lesser extent during the pulse, which for the pulse radiolysis studies was typically 10 to 20 ns. The rate constant,  $k_r$ , for electron recombination with positive ions, in most nonpolar liquids is given by:

$$k_r = \frac{4\pi e\mu_D}{\epsilon} = 1.09 \times 10^{15} (\mu_e/\epsilon) \text{ M}^{-1}\text{s}^{-1} \quad (\text{for } \mu_e \text{ in cm}^2/\text{Vs}). \quad (7)$$

This equation is sufficiently valid that it is considered to be a law of electron dynamics.

Exceptions exist only for very high values of  $\mu_D$  (see chapter 10).

It is important to consider the magnitude of the recombination rate in studies of this type. For methane  $k_r$  is  $1.7 \times 10^{17} \text{ M}^{-1}\text{s}^{-1}$  at 93 K.[81] Thus if a concentration of ions of 0.1  $\mu\text{M}$  were

formed in the pulse, the electrons would disappear with a first half-life of 50 ps. For 2,2,4-trimethylpentane  $k_r$  is  $3.6 \times 10^{15}$ , and for a similar concentration of electrons the recombination lifetime would be a few nanoseconds. Where the electron mobility is lower the recombination rate is slower. For methylcyclohexane, where  $\mu_e = 0.07 \text{ cm}^2/\text{Vs}$ , [18]  $k_r$  is  $4 \times 10^{13} \text{ M}^{-1}\text{s}^{-1}$  and the first half-life should be about 250 ns.

Electrons have not been detected by optical absorption in alkanes in which the mobility is greater than  $10 \text{ cm}^2/\text{Vs}$ . For example, Gillis, et al. [82] report seeing no infrared absorption in pulse irradiated liquid methane at 93 K. This is not surprising since the electron mobility in methane is  $500 \text{ cm}^2/\text{Vs}$  [81] and trapping does not occur. Geminately recombining electrons have however been detected by IR absorption in 2,2,4-trimethylpentane in a subpicosecond laser pulse experiment. [83] The drift mobility in this alkane is  $6.5 \text{ cm}^2/\text{Vs}$  and the quasi-free mobility, as measured by the Hall mobility is  $22 \text{ cm}^2/\text{Vs}$  (see section VI). Thus the electron is trapped  $2/3^{\text{rds}}$  of the time.

The nature of the absorption spectra has been discussed by several authors. [78,80,84,85] Since the trapped state is not far below the conduction band, it is at least reasonable to consider that the infrared spectrum is a bound-free transition. In the study of alkane glasses at 77 K, mentioned earlier, [80] the cross sections near threshold were found to fit the Wigner [86] power-law. This supports the idea that the spectra are due to a transition from a bound S-state to a continuum P-state. The threshold binding energy at 77K was found to be 0.48 eV. From an analysis of the spectral distribution, the authors obtained ground state properties of the trapped electron. The experimental spectrum matched that derived from a simple spherical well model, suggesting that the electron resides in a cavity of radius 0.35 nm. Other studies have arrived at a similar value for the radius. For example, Ichikawa, et al. [84] obtained 0.36 nm for 3-methylpentane glass based on a model that included a short range repulsive contribution and an attractive, Born-like, medium polarization. An electron spin resonance study of solvated

electrons in deuterated 3-methylpentane glasses indicated there were an average of three molecules in the first solvation shell. A combination of spin-echo and second moment analysis gave electron to proton distances from 0.35 to 0.43 nm.[87] These studies have provided considerable insight into the nature of the trapped state and are consistent with the transport studies discussed below.

Studies of the effect of pressure on  $\mu_D$  in a series of ten hydrocarbons revealed more information about the trapped state.[34] The pressure data led to the conclusion that the partial molar volume of the electron,  $\bar{V}_e$ , is small but may be either positive or negative. Values range from +22 cm<sup>3</sup>/mol for m-xylene to -27 cm<sup>3</sup>/mol for 1-pentene. This depends on the relative magnitude of two large volume terms that make up  $\bar{V}_e$ . One is the cavity volume, a positive term, the other is the electrostriction of the solvent around the trapped electron. Whereas the electrostriction term varies considerably depending on the compressibility of the solvent, the cavity volume does not change much and the average value for the hydrocarbons is 96 cm<sup>3</sup>/mol, corresponding to a cavity radius of 0.34 nm.

Thus, from pulse radiolysis, mobility measurements, and electron reaction studies we have information on the absorption spectra, the cavity volume and the energy of the trapped or solvated state. The nature of this state seems to be an electron that is localized in a cavity in the liquid.

## **V. Reactions of Electrons**

Electron attachment to solutes in nonpolar liquids has been studied by such techniques as pulse radiolysis, pulse conductivity, microwave absorption and flash (laser) photolysis. A considerable amount of data is now available on how rates depend on temperature, pressure and other factors. Although further work is needed, some recent experimental and theoretical studies have provided new insight into the mechanism of these reactions. To begin we consider those reactions that show reversible attachment-

detachment equilibria and therefore provide both free energy and volume change information.

### A. *Electron equilibria*

Electron equilibria of the type:



have been observed for solutes that do not dissociate on attachment and have gas phase electron affinities (EA) between -1.15 eV (benzene)[88,89] and 0.3 eV (phenanthrene)[90]. Application of high pressure facilitated the studies for solutes of very negative electron affinities like toluene, benzene and butadiene. Equilibrium constants,  $K_{eq}$ , have been evaluated by conductivity methods from changes in electron mobility and from determination of both the attachment rate constants,  $k_a$ , and the detachment rate constants,  $k_d$ . Values of  $\Delta G_r$  for various solutes are

Figure 8.5

shown in Figure 8.5 for tetramethylsilane, 2,2,4-trimethylpentane, n-hexane, and supercritical ethane as solvents. It has been shown that  $\Delta G_r$  depends on the polarization energy of the product anion,  $E_{pol}(S^-)$ , and the solvation energy of the electron  $\Delta G_s(e)$  according to:

$$\Delta G_r(l) = \Delta G_r^o(g) + E_{pol}(S^-) - \Delta G_s(e) \quad (9)$$

where  $\Delta G_r^o(g)$  is derived from the electron affinity:  $\Delta G_r^o(g) = -EA - T\Delta S_r(g)$ . For all the reactions,  $\Delta G_r^o$  is lower in 2,2,4-trimethylpentane than in tetramethylpentane (TMS) partly because  $\Delta G_s(e)$  is higher in the former solvent and also because the dielectric constant is higher in 2,2,4-trimethylpentane, which makes the value of the solvation energy lower.

The further lowering of  $\Delta G_r$  for these reactions in n-hexane is due largely to the even higher value of  $\Delta G_s(e)$  in this solvent.

Equilibria of this type have been used to determine the ground state of the electron in liquids. [100] Some of the values of  $\Delta G_s(e)$  given in Table 8.1 were evaluated this way. The reaction of the electron with  $\text{CO}_2$  was used to measure  $\Delta G_s(e)$  for hexamethyldisiloxane and bis(trimethylsilyl)methane. The electron mobility in these liquids is unusually high and  $V_0$  is therefore expected to be the same as  $\Delta G_s(e)$ . For hexamethyldisiloxane  $\Delta G_s(e)$  was found to be  $-0.70$  eV and that for bis(trimethylsilyl)methane to be  $-0.66$  eV. (see Table 8.1)

These equilibria reactions occur with large decreases in both volume and entropy. Volume changes range from  $-80$  to  $-300$   $\text{cm}^3/\text{mol}$  depending on the solute and pressure. These volume changes,  $\Delta V_r$ , are associated with the electrostriction of the solvent around the product anion,  $V_{el}(\text{ion})$ , and to some extent with a contribution of the partial molar volume of the electron,  $\bar{V}(e)$ . Thus:

$$\Delta V_r = V_{el}(\text{ion}) - \bar{V}(e) \quad (10)$$

Values of  $\bar{V}(e)$  are small compared to the overall volume changes (see Section IV). However, magnitudes of  $\Delta V_r$  were found to be much larger than could be accounted for using the classical expression for  $V_{el}(\text{ion})$ : [101]

$$V_{el}(\text{ion}) = -(e^2/2R_{ion})(1/\epsilon^2)(d\epsilon/dP) \quad (11)$$

To account for the difference between experiment and theory, Schwarz suggested that electrostriction includes the formation of a glassy shell of 7 to 9 solvent molecules around the ion. [102] This phase transition provides a substantial density increase and the observed volume changes can then be accounted for.

These attachment-detachment equilibria (Eq. 8) shift to the right with increasing pressure and to the left with increasing temperature. Thus the free energies decrease with pressure and increase with temperature. These effects are related to the solvent compressibility, which increases with pressure and decreases with temperature. The entropy contribution is less at high pressure but increases with temperature. Because both entropy and volume changes are due to electrostriction of the solvent, these quantities are related by:

$$\Delta S_{el}(\text{ion}) = (\alpha/\chi_T) \Delta V_{el}(\text{ion}), \quad (12)$$

where  $\alpha$  is the coefficient of thermal expansion and  $\chi_T$  the isothermal compressibility.

Electron attachment equilibria have also been observed in supercritical ethane. The equilibrium constants are generally smaller than in liquids and consequently  $\Delta G_r$  is higher. Thus, as shown in Figure 8.5,  $\Delta G_r$  for attachment to  $\text{CO}_2$  is higher in ethane at all pressures than in either TMS or 2,2,4-trimethylpentane liquids. This is mainly a consequence of the lower density of the solvent that results in less polarization energy for the anion. However, the continuum model of Born is no longer correct for evaluating the polarization energy because of the significant density augmentation around the ions in supercritical nonpolar fluids. Instead a compressible continuum model that takes this effect into account must be used. [99,103] In the case of a supercritical solvent like ethane the free energy of attachment to a solute changes rapidly with pressure, particularly near critical densities where the compressibility of the fluid changes rapidly. Thus as the pressure increases the values of  $\Delta G_r$  for attachment to  $\text{CO}_2$ , pyrimidine and pyrazine decrease. The equilibria in supercritical ethane could only be observed over the pressure ranges indicated in the figure for these solutes.

The volume changes,  $\Delta V_r$ , for attachment to solutes in supercritical ethane can be extremely large and they are always negative. For pyrazine as a solute, values of  $\Delta V_r$

range from  $-1.0$  to  $-45$  liters/mole, depending on temperature and pressure. The largest changes are found at the densities where the compressibility is the largest at each temperature. These changes are mostly due to electrostriction of the solvent around the ion formed and are predicted quite well by the compressible continuum model. Generally, the density augmentation around an ion in a supercritical fluid extends to a radial distance of 1 nm.

### B. Attachment rates

In nonpolar liquids bimolecular electron attachment rate constants,  $k_a$ , are much larger than those for conventional reactions of ions or radicals. This is in part related to the high mobility of electrons in these liquids; but various other factors, like  $V_0$ , the kinetic energy of the electron, and dipole moment of the solute are important as well. These and other factors are examined below and also the dependence of  $k_a$  on the energy gap,  $\Delta G_r$ , in representative liquids is also shown and discussed.

It is natural to conclude that the high rate constants for electron attachment reactions in nonpolar liquids are associated with the high mobility of electrons. Early studies [96,104,105] of attachment to biphenyl and  $SF_6$  emphasized the dependence of  $k_a$  on mobility. This relationship is apparent if the expression for the rate constant for a diffusion controlled reaction:

$$k_D = 4\pi R_e D_e \quad (13)$$

is combined with the Einstein relation:

$$D_e = \mu_D k_B T/e \quad (14)$$

then:

$$k_D = 4\pi R_e \mu_D k_B T/e \quad (15)$$

In the solvents ethane, propane, and hexane a reaction radius,  $R_e$ , of 1.4 nm was found for attachment to  $SF_6$ . This is close to the theoretical maximum radius for electron attachment in the gas phase.[106]

Modern theory suggests that rates of electron transfer reactions depend on the potential energy difference.[107] For electron attachment reactions in solution that difference is given by the difference in energy of reactants, in this case the electron plus solute, and the product anion (see Eq. 9). Since this theory works so well for electron transfer, it is interesting to examine the dependence of rates on  $\Delta G_r(l)$  for electron

Figure 8.6

attachment reactions; such a plot for cyclohexane as solvent is shown by Fig 8.6. For one of the solutes, difluorobenzene,  $\Delta G_r(l)$  is known from equilibrium studies. For the other solutes  $\Delta G_r(l)$  was calculated using Eq. 9. Values of rate constants and electron affinities are from references given in the figure legend. The continuum model of Born:

$$E_{pol}(S^-) = -\frac{e^2}{2R_s} \left(1 - \frac{1}{\epsilon}\right) \quad (16)$$

was used to calculate  $E_{pol}(S^-)$ , where the radius of the anion,  $R_s$ , was calculated from the molar volume of the solute. Many of the rates for cyclohexane are close to  $3 \times 10^{12} M^{-1}s^{-1}$  (dotted line in Fig. 8.6). Since the room temperature electron mobility in cyclohexane is  $0.22 \text{ cm}^2/Vs$ , [19] this rate corresponds to a reaction radius of 0.72 nm, assuming equation 15 applies. The lack of dependence on the exothermicity,  $\Delta G_r(l)$ , for most of the reactions included in Fig 8.6 indicates that the rate is determined by the rate of diffusion of the electron to the solute.

A plot of the attachment rate in cyclohexane versus simply the electron affinity of the solute, shown in a paper by Christophorou, [116] is similar to Fig 8.6 in appearance. Christophorou concluded that for solutes with  $EA > 0$ ,  $k_a$  is close to the diffusion controlled rate. The similarity in plots is not surprising since for many of the larger solute molecules the polarization energy is nearly the same and thus changes in  $\Delta G_r(l)$  are proportional to changes in EA. Christophorou suggests that the rate constant drops off to very low values when  $EA < -0.9$  eV.

Some reactants have rate constants higher than  $3 \times 10^{12} \text{ M}^{-1} \text{ s}^{-1}$ ; examples are nitrobenzene and o-dinitrobenzene. These two compounds have large dipole moments of 4.1 and 6.1 Debye, respectively, and it has been shown [110] that rate constants in cyclohexane increase with dipole moment because the reaction radius increases. That dependence is given by: [117]

$$R_e^{-1} = \int_{r_c}^{\infty} \frac{\exp[U(r)/k_B T]}{r^2} dr \quad (17)$$

where  $U(r)$  is a function of the dipole moment and  $r_c$  the hard core radius of the reactant pair. Diffusion rates calculated with Eq. 15 agree with the experimental values for a series of nitrobenzenes when Eq. 17 is used to calculate  $R_e$ . [110]

Many of these attachment reactions are also diffusion controlled in other solvents of low electron mobility like for example n-hexane. It has been suggested that this is the case for all solvents for which  $\mu_D < 1 \text{ cm}^2/\text{Vs}$ . [118] For this to be true the rate constant  $k_a$  should scale as the mobility. For hexane the rate constants for attachment to solutes like biphenyl, naphthalene and difluorobenzene are close to  $1 \times 10^{13} \text{ M}^{-1} \text{ s}^{-1}$  or 1/3rd the value in cyclohexane. The mobility in n-hexane is approximately 1/3rd that in cyclohexane; [2] thus  $k_a$  scales with  $\mu_D$  for these two solvents.

An interesting example of a diffusion controlled reaction is electron attachment to SF<sub>6</sub>. Early studies showed that in *n*-alkanes  $k_a$  increases linearly with  $\mu_e$  over a wide range of mobilities from 10<sup>-3</sup> to 1 cm<sup>2</sup>/Vs.[119] Another study of the effect of electric field ( $E$ ) showed that in ethane and propane  $k_a$  is independent of  $E$  up to approximately 90 kV/cm, but increases at higher fields. [105] This field is also the onset of the supralinear field dependence of the electron mobility.[120] Thus over a wide range of temperature and electric field the rate of attachment to SF<sub>6</sub> remains linearly dependent on the mobility of the electron,  $\mu_D$ , as required by Eq. 15.

Diffusion is not always rate determining of course. Exceptions shown in Figure 8.6 are oxygen and perfluoromethylcyclohexane for which the rate constants are below the diffusion rate; these are considered in more detail below. The dependence of  $k_a$  on electron mobility also breaks down if the mobility  $> 10$  cm<sup>2</sup>/Vs. This was noted early on for the reaction of the electron with biphenyl. [104,121]

Figure 8.7

Many attachment reactions have been studied in 2,2,4-trimethylpentane, a liquid for which  $\mu_D$  is 6.6 cm<sup>2</sup>/Vs at room temperature. Attachment rate constants for many solutes in 2,2,4-trimethylpentane are shown in Figure 8.7 plotted versus  $\Delta G_r(I)$ . The dotted line shows the diffusion rate for the radius of 0.72 nm, derived for cyclohexane. In 2,2,4-trimethylpentane only a few solutes, like SF<sub>6</sub>, C<sub>6</sub>F<sub>6</sub> and the metal carbonyls, come close to the diffusion rate.

The attachment rate constants for the solvent tetramethylsilane (TMS), in which the electron mobility is 100 cm<sup>2</sup>/Vs, are shown in Fig 8.8. The solutes include those listed

Figure 8.8

in a recent compilation by Nishikawa [2] plus pyrimidine and C<sub>60</sub> from recent studies.[93,122] The values of  $k_a$  range over four orders of magnitude, nevertheless some

conclusions become apparent. For large energy gaps  $k_a$  is close to  $10^{14} \text{ M}^{-1}\text{s}^{-1}$ , with the exception of benzoquinone, duroquinone and  $\text{O}_2$  which are special cases (see below). The diffusion rate, shown by the dotted line, was calculated using the value of  $R_e = 0.72 \text{ nm}$  suggested for cyclohexane. None of these reactions occurs at the diffusion rate in TMS. For moderate energy gaps ( $\Delta G_r = -0.7 \pm 0.3 \text{ eV}$ )  $k_a$  tends to be around  $10^{13} \text{ M}^{-1}\text{s}^{-1}$ . When  $\Delta G_r$  is close to zero much lower rate constants are observed.

The value of  $k_a$  for attachment to  $\text{SF}_6$  given in Fig 8.8 is  $2.1 \times 10^{14} \text{ M}^{-1}\text{s}^{-1}$ . This reaction has also been studied in other high mobility liquids including methane ( $\mu_D = 400 \text{ cm}^2/\text{Vs}$ ), argon ( $\mu_D = 400 \text{ cm}^2/\text{Vs}$ ), and xenon ( $\mu_D = 2000 \text{ cm}^2/\text{Vs}$ )[127-129] and the rate constant is nearly constant at  $3 \pm 1 \times 10^{14} \text{ M}^{-1}\text{s}^{-1}$ . This has been explained by Warman [106] and others as due to the fact that the residence time,  $\tau_D$ , of an electron within a reaction radius,  $R_e$ , is short compared to the attachment time,  $\tau_A$ . Thus rate constants would be expected to fall off with increasing mobility according to the equation:

$$k_a = \frac{4\pi R_e D}{1 + \tau_A / \tau_D} \quad (18)$$

At high enough mobility, since  $\tau_D$  is  $R_e^2/2D$ ,  $k_a$  reaches a constant value of  $2\pi R_e^3/\tau_A \cong 3 \times 10^{14} \text{ M}^{-1}\text{s}^{-1}$ , which explains the near constant rate for attachment to  $\text{SF}_6$  observed in liquids of high mobility.

Figures 8.7 and 8.8 show that rate constants are mostly below the diffusion limit. Some rates are a few orders of magnitude lower and these reactions have been interpreted as dependent on the energy gap. Attachment to  $\text{O}_2$  is a case in point.[123] Like many of these reactions this is a non-dissociative attachment reaction. As pointed out by Henglein,[130,131] attachment to  $\text{O}_2$  is most favorable when the energy gap is small. As can be seen in Figures 8.6 - 8.8,  $\Delta G_r$  is between  $-2.6$  and  $-2.0 \text{ eV}$  for these solvents and

thus the reaction is unfavorable at room temperature. Any decrease in the gap would be expected to increase the rate. The positive activation energy of approximately 2 kcal/mol for this reaction in most solvents can be accounted for in this way. As the temperature increases the density decreases causing the energy level of the electron to decrease and the value of  $E_{\text{pol}}(\text{O}_2^-)$  to increase thus narrowing the energy gap. The effect of increasing pressure on this reaction is of interest, since increasing pressure causes the density to increase, the energy levels of the electron increase and the value of  $E_{\text{pol}}(\text{O}_2^-)$  decreases. Thus the energy gap increases with increasing pressure. Preliminary studies show that the rate of attachment to  $\text{O}_2$  in n-pentane as solvent decreases a factor of two in 1 kbar. [132] The attachment rate to  $\text{O}_2$  has also been studied in liquid argon and xenon. [127] The rate decreases with increasing field or, since the field increases the average electron energy, the rate decreases as the kinetic energy of the electrons increases. Thus at higher fields there is more energy available for the reaction and the rate shows down.

There is a class of solutes, including ethylbromide,  $\text{N}_2\text{O}$ ,  $\text{C}_2\text{HCl}_3$  and certain fluoroalkanes, that show negative activation energies for attachment in liquids like TMS and neopentane. [19] [123] For ethylbromide the rate constant of electron attachment in TMS is  $4.2 \times 10^{10}$  at 23 °C. This is point 14 on Figure 8.8. Lowering the temperature causes the energy level of the electron,  $V_0$ , to increase and the polarization energy of the anion  $E_{\text{pol}}(\text{S}^-)$  to decrease. Thus lowering the temperature increases the energy gap between the electron energy level and the energy of the ion in solution and the rate increases. For neopentane as solvent the effect is similar except the electron energy level is higher making the gap larger and at 24 °C  $k_a$  is  $3.4 \times 10^{11} \text{ M}^{-1}\text{s}^{-1}$ , an order of magnitude larger than in TMS. The rate reaches a maximum in 2,2,4-trimethylpentane where  $k_a$  is  $6.3 \times 10^{12} \text{ M}^{-1}\text{s}^{-1}$  at 23 °C (point 14 in Figure 8.7) because the electron level is even higher. Thus the rate increases as the energy gap increases. In the gas phase this reaction shows a

maximum in the attachment rate for an electron energy of 0.76 eV. [133] This value was used for  $\Delta G_r(g)$  in calculating  $\Delta G_r(l)$ . In TMS  $\Delta G_r(l)$  turns out to be +0.32 eV, or this vertical attachment reaction is unfavorable. In 2,2,4-TMP  $\Delta G_r(l)$  is close to zero, or in terms of the electron redox level picture of Henglein [134], the occupied donor level (electron in the solvent) matches the unoccupied acceptor level (ethyl bromide). But the rate constant is less in cyclohexane,  $2 \times 10^{12} \text{ M}^{-1}\text{s}^{-1}$  at 23 °C, where the electron level is even higher. This is explained by the fact that the reaction is limited by the diffusion rate, which should be somewhat less than the line in Figure 8.6 because of a smaller reaction radius for this solute.

The explanation of the negative activation energies for attachment to  $\text{N}_2\text{O}$ ,  $\text{C}_2\text{HCl}_3$  [19] and perfluorocyclobutane [123] in TMS is similar to that for ethylbromide above. These molecules exhibit maxima for electron attachment in the gas phase at 2.2 eV, [135] 0.4 eV, [136] and 0.35 eV, [137] respectively. Thus rates are expected to increase as the energy gap increases. However, in 2,2,4-TMP and n-hexane the attachment rates show normal Arrhenius behavior. For these solvents the ratio  $k_a/\mu_D$  is constant over a range of temperatures indicating the reaction becomes diffusion limited as was the case for ethylbromide in cyclohexane. Other perfluoroalkanes like *n*- $\text{C}_5\text{F}_{12}$  and *n*- $\text{C}_6\text{F}_{14}$  are reported to show maxima as is seen for cyclo- $\text{C}_4\text{F}_8$ . [138]

Carbon dioxide reacts in a manner similar to the solutes discussed above in that as the energy gap increases the rate of attachment increases. However, unlike the other solutes this reaction is reversible in solution and the equilibrium:



has been studied in several nonpolar liquids as well as in supercritical ethane. Thus, not only have attachment rates,  $k_a$ , been measured, but also values of the free energy of

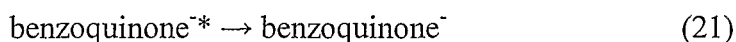
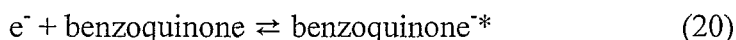
reaction,  $\Delta G_r$ , are available. The rate constants,  $k_a$ , for this reaction, obtained at various temperatures and pressures in several fluids: TMS, 2,2,4-trimethylpentane, dimethylbutane and supercritical ethane,[126,139] are plotted in Figure 8.9. In liquids the rate constant is independent of temperature at any

Figure 8.9

pressure but increases with pressure. The increase in rate with pressure can be explained by the increase in electron energy level [39] and the increase in stability of the ion with pressure that causes the energy gap to increase. As shown in figure 8.9  $\log k_a$  is linearly dependent on  $\Delta G_r$  and  $k_a$  increases about three orders of magnitude as the energy gap increases by 0.4 eV.

The reaction of electrons with p-benzoquinone is an unusual case. A conductivity study showed that the reaction is slow at room temperature in TMS and neopentane and the activation energies are negative. [140] The energy gaps are large:  $\Delta G_r(l)$  is  $-2.3$  eV in TMS and  $-2.44$  eV in neopentane, indicating possible inverted behavior. However, in 2,2,4-TMP  $\Delta G_r(l)$  is even lower,  $-2.58$  eV and the rate of attachment is fast. In cyclohexane, n-pentane, and n-hexane, where the electron levels are high, the reaction appears to be diffusion limited. The results were explained by assuming an equilibrium

with an excited state of the anion:



The excited state lies 2.07 eV above the ground state, thus there is sufficient energy available in all solvents to reach this state. The kinetic analysis indicated that the attachment rate is fast in all solvents. In TMS, neopentane, and 2,2,4,4-tetramethylpentane the energy levels of the electron

are low enough that the reverse reaction, autodetachment from the excited anion, occurs with small activation energy.

Recently the excited state of benzoquinone anion was detected both by absorption and fluorescence. [141] The lifetime of the excited state in 2,2,4-trimethylpentane is  $\approx 120$  ns or  $k_{21} = 8 \times 10^6 \text{ s}^{-1}$ . If it is assumed that the lifetime is similar in the other nonpolar solvents then the results of the two studies may be combined to evaluate the detachment rate from the excited anion. At room temperature this calculation gives  $k_{-20} = 6 \times 10^8 \text{ s}^{-1}$  in TMS, thus detachment readily competes with deactivation of the excited state of benzoquinone anion. The latter process includes internal conversion as well as fluorescence. In 2,2,4,4-tetramethylpentane, where the activation energy for detachment is 0.41 eV,  $k_{-20}$  is  $4 \times 10^6 \text{ s}^{-1}$  and some autodetachment occurs along with fluorescence. In solvents like n-pentane, n-hexane and cyclohexane the activation energies for detachment are much higher, because the electron energy levels are higher, and the reaction proceeds directly to benzoquinone anion at the diffusion rate.

For attachment to  $\text{CO}_2$  the rate constant clearly shows a dependence on  $\Delta G_r(l)$ . However, for attachment to other solutes like aromatics the dependence on  $\Delta G_r(l)$  is not yet clear. Questions remain like what is the role of reorganization energy, which can be large even in nonpolar solvents; [142] it was pointed out earlier that there is considerable density augmentation around the negative ions formed in attachment reactions. For solvents like TMS, rates maximize for values of  $\Delta G_r(l)$  near  $-0.7$  eV; what rate is to be expected for large values of  $-\Delta G_r(l)$ ? Is the high rate observed for  $\text{C}_{60}$  typical or the low rate for quinones more typical? Further study is needed to resolve these questions.

## **VI Transport Properties**

*A. Quasi-free mobility.* The drift mobility of electrons in nonpolar liquids ranges from high values such as that for liquid xenon of  $2000 \text{ cm}^2/\text{Vs}$  to low values like that for tetradecane of

0.02 cm<sup>2</sup>/Vs. It has often been suggested that the mobility is high for symmetrical molecules and low for straight chain molecules like n-alkanes. Inspection of Table 8.2 shows that liquids with

Table 8.2

symmetrical molecules are indeed at the top of the list. However, other less symmetrical molecules like *bis*-trimethylsilylmethane and 2,2,4,4-tetramethylpentane also show high drift mobility. A more important factor may be the existence of many methyl groups in the molecule. In any case, for liquids for which  $\mu_D > 10$  cm<sup>2</sup>/Vs, the electron is considered to be quasi-free.

This is supported by the Hall mobility studies, as discussed below.

The mobility of quasi-free electrons has recently been explained by the deformation potential theory. Originally from solid-state physics, this theory was applied by Basak and Cohen to liquid argon.[68] The theory assumes that scattering occurs when the electron encounters a change or fluctuation in the local density which results in a potential change. The potential is assumed to be given in terms of  $dV_0/dN$ ,  $d^2V_0/dN^2$ , etc. The formula they derived for the mobility is:

$$\mu_D = \frac{2e\hbar^4 \sqrt{2\pi} (m_e / m^*)^{5/2}}{3m_e^{5/2} (k_B T)^{1/2} k_B N^2 \{V_0'^2 T \chi_T + V_0''^2 \beta / k_B + \dots\}}, \quad (22)$$

Where  $\chi_T$  is the isothermal compressibility and  $m^*$  the effective mass of the electron. A similar expression was derived by Berlin, et al.[144] Equation 22 was latter shown to account for many of the features of the density dependence of the mobility in Ar, Kr, and Xe.[66] Namely, it predicts a minimum in the mobility near the critical density and it correctly predicts a maximum in the mobility at the density at which  $V_0$  is a minimum; i.e. when  $dV_0/dN = 0$  (compare Figures 8.3 and 8.10). Scattering in these fluids is weakest at this

Figure 8.10

density. At higher densities a decrease in mobility is predicted as is observed experimentally. Although the general features of the experimental mobility are reproduced, the predicted values of  $\mu_D$  around the minimum near  $N_C$  are much too small, largely because  $\chi_T$  for the fluids are very large in this region. Arguing that electron-medium interactions are relatively short-ranged, Nishikawa suggested that  $\chi_T$  be replaced by the adiabatic compressibility.[147] This greatly improved the agreement at these densities for Ar.

Since these papers were published, accurate values of  $V_0$  in argon have been obtained by the field ionization technique[60,61] as described in section III. Also the effective mass,  $m^*$ , of the electron in argon is now available from theory[148](see Section VI-E). Previous workers had taken  $m^* = m_e$ . As a test of equation 22 the mobility in argon was recalculated here using these new data. The adiabatic compressibility was used and the value of  $\beta$  was obtained by making both sides of equation 22 equal at the density at which  $V_0$  is a minimum. Figure 8.10 shows that this calculated mobility compares well with the experimental data of Jahnke, et al.[145] This theory has also been shown to predict quite well the density dependence of the mobility in xenon. [149]

This theory has also been used to predict mobility for molecular liquids. Neopentane and TMS are liquids that exhibit maxima in the electron mobility at intermediate densities.[46] These maxima occur at the same density at which  $V_0$  is a minimum, in accordance with the Basak-Cohen theory. The drift mobility in TMS has been measured as a function of pressure to 2500 bar.[150] The observed relative experimental changes of mobility with pressure are predicted quite well by the Basak-Cohen theory; however the predicted value of  $\mu_D$  is 2.5 times the experimental value at 1 bar and 295K. In this calculation the authors used  $\chi_T$  to evaluate the mobility. This is reasonable in this case since for liquids there is little difference between the adiabatic and isothermal compressibilities. A similar calculation for neopentane showed that the Basak-Cohen theory predicted the Hall Mobility of the electron quite well for temperatures

between 295 and 400K.[151] Itoh, et al.[152] extended the theory to mixtures taking concentration fluctuations into account, but found the data for TMS –neopentane mixtures were best fit if only density fluctuations were considered.

Other theories have been proposed in recent years to account for the mobility of quasi-free electrons. Borghesani studied the field dependence of the mobility in Ar-Kr and Ar-Xe mixtures and found the results disagreed with the deformation potential model.[153] Instead the results could be described by a gas-kinetic model, if concentration dependent scattering cross sections were used. Atrazhev, et al.[154] used pseudopotential theory and similarly derived density dependent scattering lengths, which varied from negative values at low density to positive values at high density. Their theory qualitatively describes the density dependence of the mobility in Ar, Kr, and Xe. Naveh and Laikhtman[155] introduced scattering from longitudinal-acoustic phonons into the deformation potential framework. Their theory gave excellent agreement with experimental results for Ar for densities from 0.8 to  $11.2 \times 10^{21} \text{ cm}^{-3}$ . A different approach was used by Hsu and Chandler[146] who used Feynman's polaron theory[156] for the mobility and a pseudopotential consisting of attractive and repulsive parts. These two terms counteract at some intermediate density and result in a peak in the mobility. Their calculation for Ar is shown as the dashed line in figure 8.10.

The deformation potential model seems to provide a suitable framework to understand the quasi-free electron mobility in nonpolar liquids. Already several extensions or modifications on this theory have been proposed and the dependence on temperature and pressure seem to be adequately explained. But several authors have taken different approaches to the problem showing that a consensus in our understanding has not yet been reached.

*B. Trapped State Transport.* For many nonpolar liquids the electron drift mobility is less than  $10 \text{ cm}^2/\text{Vs}$ , too low to be accounted for in terms of a scattering mechanism. In these liquids

electrons are trapped as discussed in Section IV. Considerable evidence now supports the idea of a two-state model in which equilibrium exists between the trapped and quasi-free states:



The magnitude of the mobility then depends on the value of the quasi-free mobility in such liquids multiplied by the fraction of time the electron is quasi-free, since the trapped electron is relatively immobile. Thus:

$$\mu_D = \mu_{\text{qf}} \frac{[e_{\text{qf}}^-]}{[e_{\text{qf}}^-] + [e_{\text{tr}}^-]} = \mu_{\text{qf}} \frac{1}{1 + K_{23}} \quad (24)$$

This equilibrium depends on many factors like  $V_0$ ,  $\Delta G_{\text{soln}}(e^-)$ , temperature, and pressure.

Differences in these and other factors are presumed to account for the wide range of mobilities observed (see Table 8.2).

Studies of the effect of pressure on  $\mu_D$  for nonpolar liquids provided support for the two-state model. Pressure affects the position of the equilibrium (23) because of the volume change associated with trapping of the electron,  $\Delta V_{\text{tr}}$ . These volume changes were deduced from changes in  $\mu_D$  with pressure. For n-alkanes[157] as well as some alkenes[158] the mobility decreases with pressure, as shown in figure 8.11 for n-hexane and 1-pentene.

Figure 8.11

These changes in  $\mu_D$  led to values of  $\Delta V_{\text{tr}}$  equal to  $-22$  and  $-27$   $\text{cm}^3/\text{mol}$  for n-hexane and 1-pentene, respectively. The negative volume changes are due to the role of electrostriction[160] of the solvent around the trapped electron and the electrostriction volume,  $V_{\text{el}}$ , is a function of the isothermal compressibility  $\chi_T$  of the liquid.

For certain liquids like cyclohexene,[158] o-xylene and m-xylene[159] the mobility increases with increasing pressure (see Figure 8.11). These results provided the key to understand the two-state model of electron transport. In terms of the model  $\Delta V_{\text{tr}}$  is positive; for

example, for o-xylene  $\Delta V_{tr}$  is  $+21 \text{ cm}^3/\text{mol}$ . Since electrostriction can only contribute a negative term, it follows that there must be a positive volume term which is the cavity volume,  $V_{cav}(e)$ . The observed volume changes,  $\Delta V_{tr}$ , are the volume changes for reaction 23. These can be identified with the partial molar volume,  $\bar{V}_e$ , of the trapped electron, since the partial molar volume of the quasi-free electron, which does not perturb the liquid, is assumed to be zero. Then the partial molar volume is taken to be the sum of two terms, the cavity volume and the volume of electrostriction of the trapped electron:

$$\Delta V_{tr} \cong \bar{V}_e = V_{cav}(e) + V_{el}(e) \quad (25)$$

Whether  $\bar{V}_e$  is positive or negative depends on the relative value of the two terms in Eq. 25. Ten hydrocarbons were studied and the cavity volume term found to be relatively constant at  $96 \pm 18 \text{ cm}^3/\text{mol}$ . The electrostriction term varies, however, with the compressibility of the liquid. The compressibilities of the xylenes are approximately one-third that for 1-pentene. Thus the cavity volume term dominates for the xylenes and  $\Delta V_{tr}$  is positive. The  $V_{el}$  term dominates for 1-pentene and the n-alkanes and  $\Delta V_{tr}$  is negative.

The main experimental effects are accounted for with this model. Some approximations have been made; a higher-level calculation is needed which takes into account the fact that the charge distribution of the trapped electron may extend outside the cavity into the liquid. A significant unknown is the value of the quasi-free mobility in low mobility liquids. In principle Hall mobility measurements (see section VI-C) could provide an answer but so far have not. Berlin, et al. estimated a value of  $\mu_{qf} = 27 \text{ cm}^2/\text{Vs}$  for hexane.[144] Others have suggested values around  $100 \text{ cm}^2/\text{Vs}$ . Mozumder introduced the modification that motion of the electron in the quasi-free state may be in part ballistic, meaning there is very little scattering of the electron while in the quasi-free state.[161]

Thus, considerable support exists to support the two-state model of electron transport. The magnitude of the mobility is dependent on many factors including  $V_0$ ,  $\mu_{\text{qf}}$ ,  $\Delta G_{\text{soln}}(e)$ , temperature, pressure, and other factors. Presumably differences in these factors can explain the wide range of mobilities observed for nonpolar liquids. For example, Mozumder has recently related  $\mu_{\text{D}}$  to  $G_{\text{fi}}$  for a series of hydrocarbons through the thermalization distance.[162] The fact that the mobility of trans-2-butene is approximately 100 times lower than that of cis-2-butene ( $2.2 \text{ cm}^2/\text{Vs}$ )[163] is still quite surprising.

*C. Hall Mobility.* Measurements of the Hall mobility of electrons in nonpolar liquids are few in number but those that have been made provide information about the transport processes that is not available from drift measurements alone. The Hall mobility,  $\mu_{\text{H}}$ , is obtained by measuring the deflection of electrons by a magnetic field while they are drifting in an electric field. Since the deflection occurs only while the electrons are quasi-free,  $\mu_{\text{H}}$ , is a measure of  $\mu_{\text{qf}}$ . Measurements of  $\mu_{\text{H}}$  that have been done are for liquids of high drift mobility. The results for liquid argon[164] and xenon[165] show that  $\mu_{\text{H}}$  is approximately equal to  $\mu_{\text{D}}$  near the respective triple points. The results for TMS indicate the ratio  $\mu_{\text{H}}/\mu_{\text{D}}$  is close to unity over a large temperature range from 295 to 437 K.[166] For neopentane  $\mu_{\text{H}}$  is quite comparable to  $\mu_{\text{D}}$  at temperatures from 293 K to 413 K; however near the critical temperature, 434 K, the ratio  $\mu_{\text{H}}/\mu_{\text{D}}$  is about five, suggesting there are localized states produced by density fluctuations in neopentane at this temperature.[151,167] This effect is similar to the localization in clusters observed in xenon near the critical density (see above). For 2,2-dimethylbutane  $\mu_{\text{H}}$  is  $12 \text{ cm}^2/\text{Vs}$  and for 2,2,4,4-tetramethylpentane  $\mu_{\text{H}}$  is  $32 \text{ cm}^2/\text{Vs}$  at 293 K.[168] These values are comparable to the values of the drift mobility for these compounds (see Table 8.2). For 2,2,4-trimethylpentane  $\mu_{\text{H}}$  is 3.5 times  $\mu_{\text{D}}$  at room temperature, indicating trapping occurs in this liquid, which is consistent with the observation of the solvated electron in this liquid (see section IV).

*Diffusion Coefficient.* For molecular liquids the diffusion coefficient of the electron can be obtained from the mobility and the Einstein relation, Eq. 14. The electrons remain thermal in such liquids and the temperature,  $T$ , of the liquid can be used in Eq. 14. In liquid rare gases this is not the case if an electric field is applied, which causes the electrons to gain energy. The extent of this effect was measured for liquid argon by Shibamura, et al.[169] The energy was derived from the diffusion broadening of the electron cloud during drift of the electrons in an electric field. Values of  $D_e$  were derived and the energy,  $k_B T$ , of the electrons calculated from Eq. 14. The electron energy was found to increase from 0.1 to 0.4 eV as the electric field increased from 2 to 10 kV/cm.

*E. Effective Mass ( $m^*$ ).* Because of the lack of long range order in liquids the quasi-free electron is subjected to multiple scattering. This is taken into account by making an effective mass approximation in theoretical calculations of the mobility (see Eq. 22 and Section III). Previously, because of the lack of experimental data, the effective mass was put equal to the free electron mass. The effective mass has been evaluated[170] for some liquids from  $O_2^-$  ionization cross section spectra.[171] This procedure gave  $m^* = 0.26 m_e$  for argon at 87 K, and  $m^* = 0.27 m_e$  for TMS, 2,2-dimethylbutane and 2,2,4-trimethylpentane at 296 K. From exciton spectra Reininger, et al. determined  $m^*$  for argon to be  $0.55 m_e$  at the triple point.[172] In a similar way Reshotko, et al. determined  $m^*$  to be  $0.28 m_e$  for Xe at several densities near  $N_t$ . [173]

Recently, the effective mass of the electron has been calculated[148] within a Wigner-Seitz framework[174] for Ar, Kr, and Xe. In all three liquids  $m^*$  decreases with increasing density. At the triple point densities  $m^* = 0.6 m_e$  in argon and  $m^* = 0.3 m_e$  in xenon.

*F. Fast Negative Ions.* In some liquids the electron is trapped as a solvent negative ion yet transport occurs much faster than expected for an ion. A well documented example of this type of electronic transport is found in liquid perfluorobenzene where the electron attaches to form  $C_6F_6^-$ . [175] Although the  $V_0$  level is not known for this liquid, the anion is stable because the

electron affinity of  $C_6F_6$  is 1.1 eV and the anion is further stabilized by polarization. However, the negative ion has a mobility of  $0.018 \text{ cm}^2/\text{Vs}$ , much greater than that of the positive ion. Another example is the negative ion in liquid  $CS_2$ , which has a mobility approximately 10 times that of the positive ion.[176] In supercritical  $CO_2$  the anion also has a high mobility. At  $41^\circ\text{C}$  the solvent anion mobility is  $0.01 \text{ cm}^2/\text{Vs}$  near critical density and increases with density to  $0.015 \text{ cm}^2/\text{Vs}$  at  $0.8 \text{ g/cm}^3$ . This increase is expected for a hopping mechanism since the average distance between sites decreases as the density increases. Solute ions are reported to have a mobility of about  $0.002 \text{ cm}^2/\text{Vs}$  at this temperature in supercritical  $CO_2$ .[177]

Studies have shown that the electron mobility in aromatic liquids changes upon application of external pressure but becomes constant above 2 kbar. At low pressures the electron is trapped in a cavity as discussed for alkanes in section VI-B. Increasing the pressure causes the equilibria:



to shift to the right. The mobility observed at high pressure for toluene is  $0.06 \text{ cm}^2/\text{Vs}$ ,[178] for benzene is  $\leq 0.08 \text{ cm}^2/\text{Vs}$ ,[178] for m-xylene and o-xylene  $0.06$  and  $0.04 \text{ cm}^2/\text{Vs}$ , respectively.[159] Transport at high pressure is believed to occur by hopping:



Hopping occurs between neighboring molecules and the activation energies are small, from 0.12 to 0.15 eV for the hydrocarbons. Fast anions have also been suggested for liquid  $SF_6$ .[179] Thus several examples of this type of transport for the negative charge exist and the mobilities are comparable. More examples are expected to be found in the future.

*Positron mobility.* It is interesting to compare the properties of positive electrons, positrons, with the properties of electrons in nonpolar liquids. Values of the mobility of positrons,  $\mu_+$ , are now available for a few liquids. Early measurements for  $\mu_+$  in n-hexane ranged

from 8.5 to 100 cm<sup>2</sup>/Vs.[180,181] In a recent study the Doppler shift in energy of the 511 keV annihilation gamma ray in an electric field was utilized to measure the drift velocity. This method led to  $\mu_{\mu^+} = 53$  cm<sup>2</sup>/Vs in n-hexane and 69 cm<sup>2</sup>/Vs in 2,2,4-trimethylpentane.[182] Interestingly these values are comparable to the mobilities of quasi-free electrons in nonpolar liquids.

### Applications

This chapter would not be complete without mentioning applications of electrons in nonpolar liquids. Scientists who are very interested in the properties of electrons in these liquids are the detector physicists, working in high energy physics, gamma ray astronomy, cosmic radiation, or positron emission tomography.[183]. Ionization chambers are used in these fields to detect particles by the current signals induced by the excess electrons produced. Ideal liquids for such applications would have high free ion yields, high drift velocities, and high density. Liquid purity is important as well so that the electrons live long enough to reach the electrode.

Table 8.3

There are a variety of detectors currently in use to detect particles from neutrinos to WIMPS. Table 8.3 is a partial list of some of these that are currently in use or under construction. As noted, some utilize multi-ton quantities of liquid. The first such detector was a sampling calorimeter containing 300 liters of liquid argon.[184] Many of the detectors in use today in high energy physics experiments are of this type. They are calorimeters because the particles are totally stopped within the detector and the energy of the particles can be determined by the ionization produced in the liquid. Heavy metal plates, each a few mm thick, are introduced and the ionization is 'sampled' in the liquid between the plates. An electromagnetic calorimeter detects electrons and gamma rays. The latter create electron-positron pairs; these in turn produce lower energy gammas that create more pairs, etc. This sequence of events is called an electromagnetic shower. The D0 detector at Fermilab is an example that has been in operation

since 1991.[185] A hadron calorimeter that records signals from strongly interacting particles is often incorporated in such detectors. Calorimeters have necessarily grown as the energy of the particles in high energy physics experiments have increased. For example, the ATLAS detector at CERN is a 200 kiloton detector. Specific details about these detectors are given in the cited references. [186] To avoid the necessity of a cryogenic container some calorimeters have utilized molecular liquids like TMS[187]and 2,2,4,4-tetramethylpentane.[188]

Another type of liquid detector is the time projection chamber (TPC). Examples are ICARUS, a large liquid Ar detector,[189] and LXeGRIT.[190] These detectors determine both the energy and direction of the incoming particle or photon.[191] Liquid xenon detectors are usually smaller due to the high cost of xenon. For the purposes of gamma-ray astronomy, the scintillation of the xenon provides a trigger for an event and the direction of the particle is obtained by measuring the time required for electrons to drift to the collecting electrodes. Balloon flights by E. Aprile's group from Columbia have demonstrated the feasibility of such gamma-ray telescopes. [190]

### **Acknowledgment.**

The preparation of this review was done at Brookhaven National Laboratory and supported under contract DE-AC02-98-CH10886 with U.S. Department of Energy and supported by its Division of Chemical Sciences, Office of Basic Energy Sciences.

## References

- 1) G. R. Freeman, in *Kinetics of Nonhomogeneous Processes*, edited by G. R. Freeman (Wiley, New York, 1987), pp. 63.
- 2) M. Nishikawa, in *Handbook of Radiation Chemistry*, edited by T. Y and Y. Ito (CRC Press, Boca Raton, 1991), pp. Chapter 7.
- 3) W. F. Schmidt, *Liquid State Electronics of Insulating Liquids*. (CRC Press, Boca Raton, 1997).
- 4) A. Mozumder, *Fundamentals of Radiation Chemistry*. (Academic Press, San Diego, 1999).
- 5) L. Onsager, *Phys. Rev.* **54**, 554 (1938).
- 6) W. F. Schmidt, *Radiation Research* **42**, 73 (1970).
- 7) Y. Hoshi, M. Higuchi, H. Iso, M. Sakamoto, K. Ooyama, H. Yuta, K. Abe, K. Hasegawa, F. Suekane, N. Kawamura, M. Neichi, K. Suzuki, M. Masuda, R. Kikuchi, and K. Miyano, *IEEE Trans. Nucl. Sci.* **40**, 532 (1993).
- 8) S. S.-S. Huang and G. R. Freeman, *Can. J. Chem.* **55**, 1838 (1977).
- 9) J. M. Warman, K. D. Asmus, and R. H. Schuler, in *Advances in Chemistry Series 82*, edited by R. F. Gould (American Chemical Society, Washington, 1968), Vol. 82, pp. 25.
- 10) J.-P. Jay-Gerin, *Can. J. Chem.* **71**, 287 (1993).
- 11) S. Geer and R. A. Holroyd, *Phys. Rev. B* **46**, 5043 (1992).
- 12) B. C. LeMotais and C. D. Jonah, *Radiat. Phys. Chem.* **33**, 505 (1989).

- 13) A. Saeki, T. Kozawa, Y. Yoshida, and S. Tagawa, *Radiat. Phys. Chem.* **60**, 319 (2001).
- 14) W. M. Bartczak and A. Hummel, *Chem. Phys. Lett.* **208**, 232 (1993).
- 15) R. A. Holroyd, K. Itoh, and M. Nishikawa, *NUCL INSTRUM METH PHYS RES A* **390**, 233 (1997).
- 16) N. Gee, C. Senanayake, and G. R. Freeman, *J. Chem. Phys.* **89**, 3710 (1988).
- 17) W. F. Schmidt and A. O. Allen, *J. Chem. Phys.* **52**, 2345 (1970).
- 18) A. O. Allen and R. A. Holroyd, *J. Phys. Chem.* **78**, 796 (1974).
- 19) A. O. Allen, T. E. Gangwer, and R. A. Holroyd, *J. Phys. Chem.* **79**, 25 (1975).
- 20) M. Nishikawa, Y. Yamaguchi, and K. Fujita, *J. Chem. Phys.* **61**, 2356 (1974).
- 21) Y. Yamaguchi and M. Nishikawa, *J. Chem. Phys.* **59**, 1298 (1973).
- 22) R. A. Holroyd, P. Y. Chen, E. Stradowska, and K. Itoh, *Radiat. Phys. Chem.* **48**, 635 (1996).
- 23) R. A. Holroyd and T. K. Sham, *J. Phys. Chem.* **88**, 2909 (1985).
- 24) R. A. Holroyd, T. K. Sham, B. X. Yang, and X. H. Feng, *J. Phys. Chem.* **96**, 7438 (1992).
- 25) R. A. Holroyd and T. K. Sham, *Radiat. Phys. Chem.* **51**, 37 (1998).
- 26) W. M. Bartczak and A. Hummel, *Radiat. Phys. Chem.* **49**, 675 (1997).
- 27) L. D. A. Siebbeles, W. M. Bartczak, M. Terrissol, and A. Hummel, *J. Phys. Chem.* **101**, 1619 (1997).
- 28) R. A. Holroyd and J. M. Preses, in *Chemical Applications of Synchrotron Radiation*, edited by T.-K. Sham (World Scientific, River Edge, NJ, 2002), Vol. 12B, pp. 987.

- 29) W. M. Bartczak and A. Hummel, *J. Phys. Chem.* **97**, 1253 (1993).
- 30) M. Chybicki, *Acta Phys. Pol.* **30**, 927 (1966).
- 31) R. C. Munoz, J. B. Cumming, and R. A. Holroyd, *J. Chem. Phys.* **85**, 1104 (1986).
- 32) T. Lindblad, L. Bagge, A. Engstrom, J. Bialkowski, C. R. Gruhn, W. Pang, M. Roach, and R. Loveman, *Nucl. Inst. and Methods* **215**, 183 (1983).
- 33) A. Mozumder, *J. Phys. Chem.* **100**, 5964 (1996).
- 34) R. A. Holroyd and M. Nishikawa, *Radiat. Phys. Chem.* **64**, 19 (2002).
- 35) A. A. Balakin, I. A. Boriev, and B. S. Yakovlev, *Can. J. Chem.* **55**, 1985 (1977).
- 36) D. F. Anderson, G. Charpak, R. A. Holroyd, and D. C. Lamb, *Nucl. Inst. and Methods in Phys. Res.* **A261**, 445 (1987).
- 37) B. E. Springett, J. Jortner, and M. H. Cohen, *J. Chem. Phys.* **48**, 2720 (1968).
- 38) R. A. Holroyd, S. Tames, and A. Kennedy, *J. Phys. Chem.* **79**, 2857 (1975).
- 39) R. A. Holroyd, M. Nishikawa, K. Nakagawa, and N. Kato, *Phys. Rev. B* **45**, 3215 (1992).
- 40) B. Halpern, J. Lekner, S. A. Rice, and R. Gomer, *Phys. Rev.* **156**, 351 (1967).
- 41) R. A. Holroyd and M. Allen, *J. Chem. Phys.* **54**, 5014 (1971).
- 42) R. A. Holroyd and W. Tauchert, *J. Chem. Phys.* **60**, 3715 (1974).
- 43) R. Schiller, S. Vass, and J. Mandics, *J. Radiat. Phys. Chem.* **5**, 491 (1973).
- 44) Y. Yamaguchi, T. Nakajima, and M. Nishikawa, *J. Chem. Phys.* **72**, 550 (1979).

- 45) K. Nakagawa, K. Ohtake, and M. Nishikawa, *J. Electrostat.* **12**, 157 (1982).
- 46) R. A. Holroyd and N. E. Cipollini, *J. Chem. Phys.* **69**, 501 (1978).
- 47) A. Boriev, A. A. Balakin, and B. S. Yakovlev, *Khim. Vys. Energ.* **12**, 20 (1978).
- 48) A. F. Borghesani, G. Carugno, and M. Santini, *IEEE Trans. on Elec. Insulation* **26**, 615 (1991).
- 49) R. A. Holroyd and R. L. Russell, *J. Phys. Chem.* **78**, 2128 (1974).
- 50) R. A. Holroyd, B. K. Dietrich, and H. A. Schwarz, *J. Phys. Chem.* **76**, 3794 (1972).
- 51) Y. Nakato and H. Tsubomura, *J. Phys. Chem.* **79**, 2135 (1975).
- 52) E.-H. Bottcher and W. F. Schmidt, *J. Chem. Phys.* **80**, 1353 (1984).
- 53) R. A. Holroyd, J. M. Preses, E. H. Bottcher, and W. F. Schmidt, *J. Phys. Chem.* **88**, 744 (1984).
- 54) J. Casanovas, R. Grob, R. Sabattier, J. P. Gruelfucci, and D. Blanc, *Radiat. Phys. Chem.* **15**, 293 (1980).
- 55) J. Casanovas, R. Grob, D. Delacroix, J. P. Guelfucci, and D. Blanc, *J. Chem. Phys.* **75**, 4661 (1981).
- 56) J. S. Greever, J. B. M. Turner, and J. F. Kauffmann, *J. Phys. Chem. A* **105**, 8635 (2001).
- 57) U. Sowada and R. A. Holroyd, *J. Phys. Chem.* **84**, 1150 (1980).
- 58) U. Sowada and R. A. Holroyd, *J. Phys. Chem.* **85**, 541 (1981).
- 59) L. V. Lukin and B. S. Yakovlev, *Chem. Phys. Lett* **42**, 307 (1976).

- 60) A. K. Al-Omari and R. Reininger, *J. Chem. Phys.* **103**, 506 (1995).
- 61) A. K. Al-Omari, K. N. Altmann, and R. Reininger, *J. Chem. Phys.* **105**, 1305 (1996).
- 62) A. K. Al-Omari and R. Reininger, *J. Chem. Phys.* **103**, 4484 (1995).
- 63) K. N. Altmann and R. Reininger, *J. Chem. Phys.* **107**, 1759 (1997).
- 64) P. Stampfli and K. H. Bennemann, *Phys. Rev. A* **44**, 8210 (1991).
- 65) B. Plenkiewicz, Y. Frongillo, J.-M. Lopez-Castillo, and J.-P. Jay-Gerin, *J. Chem. Phys.* **104**, 9053 (1996).
- 66) R. Reininger, U. Asaf, I. T. Steinberger, and S. Basak, *Phys. Rev. B* **28**, 4426 (1983).
- 67) F. M. Jacobsen, N. Gee, and G. R. Freeman, *Phys. Rev. A* **34**, 2329 (1986).
- 68) S. Basak and M. H. Cohen, *Phys. Rev. B* **20**, 3404 (1979).
- 69) E. Fermi, *Nuovo Cimento* **11**, 157 (1934).
- 70) J.-M. Lopez-Castillo, Y. Frongillo, B. Plenkiewicz, and J.-P. Jay-Gerin, *Chem. Phys.* **96**, 9092 (1992).
- 71) J.-M. Lopez-Castillo and J.-P. Jay-Gerin, *Phys. Rev. E* **52**, 4892 (1995).
- 72) B. Space, D. F. Coker, Z. H. Liu, B. Berne, and G. Martyna, *J. Chem. Phys.* **97**, 2002 (1992).
- 73) B. Boltjes, C. deGraaf, and S. W. Leeuw, *J. Chem. Phys.* **98**, 592 (1993).
- 74) S. H. Simon, V. Dobrosavljevic, and R. M. Strat, *Phys. Rev. A* **42**, 6278 (1990).
- 75) S. H. Simon, V. Dobrosavljevic, and R. M. Strat, *J. Chem. Phys.* **94**, 7360 (1991).

- 76) Y. Frongillo, B. Plenkiewicz, J.-P. Jay-Gerin, and A. Jain, *Phys. Rev. E* **50**, 4754 (1994).
- 77) J. H. Baxendale, C. Bell, and P. Wardman, *J. Chem. Soc. Far. Trans. I* **69**, 776 (1973).
- 78) S. J. Atherton, J. H. Baxendale, F. Busi, and A. Kovacs, *Radiat. Phys. Chem.* **28**, 183 (1986).
- 79) H. A. Gillis, N. V. Klassen, and R. J. Woods, *Can. J. Chem.* **55**, 2022 (1977).
- 80) S. D. McGrane and S. Lipsky, *J. Phys. Chem.* **105**, 2384 (2001).
- 81) Y. Nakamura, K. Shinsaka, and Y. Hatano, *J. Chem. Phys.* **78**, 5820 (1983).
- 82) H. A. Gillis, N. V. Klassen, G. G. Teather, and K. H. Lokan, *Chem. Phys. Lett.* **10**, 481 (1971).
- 83) L. D. A. Siebbeles, U. Emmerichs, A. Hummel, and H. J. Bakker, *J. Chem. Phys.* **107**, 9339 (1997).
- 84) T. Ichikawa and H. Yoshida, *J. Chem. Phys.* **73**, 1540 (1980).
- 85) T. Kimura, N. Ogawa, and K. Fueki, *Bull. Chem. Soc. Jpn.* **54**, 3854 (1981).
- 86) E. P. Wigner, *Phys. Rev.* **73**, 1002 (1948).
- 87) L. Kevan, *Radiat. Phys. Chem.* **17**, 413 (1981).
- 88) K. Itoh and R. Holroyd, *J. Phys. Chem.* **94**, 8854 (1990).
- 89) K. Itoh, M. Nishikawa, and R. Holroyd, *J. Phys. Chem.* **97**, 503 (1993).
- 90) R. A. Holroyd, *Ber. Bunsenges Phys. Chem.* **81**, 28 (1977).
- 91) U. Sowada and R. A. Holroyd. Private communication

- 92) P. Y. Chen and R. A. Holroyd, *J. Phys. Chem.* **99**, 14528 (1995).
- 93) P. Y. Chen and R. A. Holroyd, *J. Phys. Chem.* **100**, 4491 (1996).
- 94) R. A. Holroyd, T. E. Gangwer, and A. O. Allen, *Chem. Phys. Lett.* **31**, 520 (1975).
- 95) R. A. Holroyd, R. D. McCreary, and G. Bakale, *J. Phys. Chem.* **83**, 435 (1979).
- 96) J. M. Warman, M. P. deHaas, E. Zador, and A. Hummel, *Chem. Phys. Lett.* **35**, 383 (1975).
- 97) R. A. Holroyd, M. Nishikawa, and K. Itoh, *J. Phys. Chem. B* **103**, 9205 (1999).
- 98) R. A. Holroyd, M. Nishikawa, and K. Itoh, *J. Phys. Chem. B* **104**, 11585 (2000).
- 99) M. Nishikawa, K. Itoh, and R. A. Holroyd, *J. Phys. Chem. A* **103**, 550 (1999).
- 100) R. A. Holroyd, K. Itoh, and M. Nishikawa, *Chem. Phys. Lett.* **266**, 227 (1997).
- 101) S. D. Hamann, *Physico-Chemical Effects of Pressure*. (Butterworths, London, 1957).
- 102) H. A. Schwarz, *J. Phys. Chem.* **97**, 12954 (1993).
- 103) K. Itoh, R. A. Holroyd, and M. Nishikawa, *J. Phys. Chem. A* **105**, 703 (2001).
- 104) G. Beck and J. K. Thomas, *Chem. Phys. Lett.* **13**, 295 (1972).
- 105) G. Bakale and W. F. Schmidt, *Zeit Naturforsch* **36a**, 802 (1981).
- 106) J. M. Warman, in *The Study of Fast Processes and Transient Species by Electron Pulse Radiolysis*, edited by J. H. Baxendale and F. Busi (Reidel, Dordrecht, Holland, 1982), pp. 433ff.
- 107) M. Tachiya, *J. Phys. Chem.* **97**, 5911 (1993).

- 108) M. C. Sauer and K. H. Schmidt, *Radiat. Phys. Chem.* **43**, 413 (1994).
- 109) G. Bakale, R. D. McCreary, and E. C. Gregg, *Cancer Biochem. Biophys.* **5**, 103 (1981).
- 110) G. Bakale, E. C. Gregg, and R. D. McCreary, *J. Chem. Phys.* **67**, 5788 (1977).
- 111) J. H. Baxendale, J. P. Keene, and E. J. Rasburn, *J. Chem. Soc. Far. Trans.* **70**, 718 (1974).
- 112) E. S. Chen, E. C. M. Chen, N. Sane, L. Talley, N. Kozanecki, and S. Shulze, *J. Chem. Phys.* **110**, 9319 (1999).
- 113) A. A. Christodoulides, D. L. McCorkle, and L. G. Christophorou, Report No. DOE/EV/04703--39.
- 114) A. F. Gains, J. Kay, and F. M. Page, *Trans Far. Soc* **62**, 874 (1966).
- 115) P. Kebarle and Chowdhury, *Chem. Rev.* **87**, 513 (1987).
- 116) L. G. Christophorou, *Zeitschrift fur Physikalische Chemie* **195s**, 195 (1996).
- 117) J. R.E. Weston and H. A. Schwarz, *Chemical Kinetics*. (Prentice-Hall, Englewood Cliffs, NJ, 1972).
- 118) K. Funabashi and J. L. Magee, *J. Chem. Phys.* **62**, 4428 (1975).
- 119) G. Bakale, U. Sowada, and W. F. Schmidt, *J. Phys. Chem.* **79**, 3041 (1975).
- 120) W. F. Schmidt, G. Bakale, and U. Sowada, *J. Chem. Phys.* **61**, 5275 (1974).
- 121) G. Beck and J. K. Thomas, *J. Chem. Phys.* **57**, 3649 (1972).
- 122) R. A. Holroyd. Private communication
- 123) R. A. Holroyd and T. E. Gangwer, *Radiat. Phys. Chem.* **15**, 283 (1980).

- 124) Y. S. Kang and R. A. Holroyd, *Radiat. Phys. Chem.* **20**, 237 (1982).
- 125) J. M. Warman, M. P. deHaas, and A. Hummel, in *Conduction and Breakdown in Dielectric Liquid*, edited by Goldschwartz (Delft Univ. Press, 1975), pp. 70.
- 126) M. Nishikawa, K. Itoh, and R. Holroyd, *J. Phys. Chem.* **92**, 5262 (1988).
- 127) G. Bakale, U. Sowada, and W. F. Schmidt, *J. Phys. Chem.* **80**, 2556 (1976).
- 128) G. Bakale, U. Sowada, and W. F. Schmidt, *J. Phys. Chem.* **79**, 3041 (1975).
- 129) U. Sowada, G. Bakale, K. Yoshino, and W. F. Schmidt, *Chem. Phys. Lett.* **34**, 466 (1975).
- 130) A. Henglein, *Berichte der Bunsen-Gesellschaft Phys. Chem* **79**, 129 (1976).
- 131) A. Henglein, *Can. J. Chem.* **55**, 2112 (1976).
- 132) K. Nakagawa and R. A. Holroyd. Private communication
- 133) L. G. Christophorou, *Atomic and Molecular Radiation Physics*. (Wiley-Interscience, New York, 1971).
- 134) A. Henglein, *Berichte der Bunsen-Gesellschaft Phys. Chem* **79**, 129 (1975).
- 135) W.E. Wentworth, E. Chen, and R. Freeman, *J. Chem. Phys.* **55**, 2075 (1971).
- 136) R. P. Blaunstein and L. G. Christophorou, *J. Chem. Phys.* **49**, 1526 (1968).
- 137) L. G. Christophorou, D. L. McCorkle, and D. Pittman, *J. Chem. Phys.* **60**, 1183 (1974).
- 138) R. Holroyd, in *The Liquid State and Its Electronic Properties*, edited by E. E. Kunhardt, L. G. Christophorou, and L. H. Luessen (Plenum Press, New York, 1987), Vol. 193, pp. 221.
- 139) S. Ninomiya, K. Itoh, M. Nishikawa, and R. Holroyd, *J. Phys. Chem.* **97**, 9488 (1993).

- 140) R. A. Holroyd, *J. Phys. Chem.* **86**, 3541 (1982).
- 141) A. R. Cook, L. A. Curtiss, and J. R. Miller, *J. Am. Chem. Soc.* **119**, 5729 (1997).
- 142) D. V. Matyushov and R. Schmid, *Molecular Physics* **84**, 533 (1995).
- 143) A. Astbury, R. K. Keeler, Y. Li, P. R. Poffenberger, and L. P. Robertson, *Nuc. Inst. and Methods in Phys. Research A* **305**, 376 (1991).
- 144) Y. A. Berlin, L. Nyikos, and R. Schiller, *J. Chem. Phys.* **69**, 2401 (1978).
- 145) J. A. Jahnke, L. Meyer, and S. A. Rice, *Phys. Rev. A* **3**, 734 (1971).
- 146) D. Hsu and D. Chandler, *J. Chem. Phys.* **93**, 5075 (1990).
- 147) M. Nishikawa, *Chem. Phys. Lett.* **114**, 271 (1985).
- 148) B. Plenkiewicz, Y. Frongillo, P. Plenkiewicz, and J.-P. Jay-Gerin, *J. Chem. Phys.* **94**, 6132 (1991).
- 149) R.A. Holroyd, M. Nishikawa, K. Itoh, *J. Phys. Chem.* submitted
- 150) R. C. Munoz and R. A. Holroyd, *J. Chem. Phys.* **84**, 5810 (1986).
- 151) R. C. Munoz and G. Ascarelli, *J. Phys. Chem.* **88**, 3712 (1984).
- 152) K. Itoh, M. Nishikawa, and R. A. Holroyd, *Phys. Rev. B* **44**, 680 (1991).
- 153) A. F. Borghesani, D. Iannuzzi, and G. Carugno, *J. Phys.: Condens. Matter* **9**, 5057 (1997).
- 154) V. M. Atrazhev and I. T. Iakubov, *J. Chem. Phys.* **103**, 9030 (1995).
- 155) Y. Naveh and B. Laikhtman, *Phys. Rev. B* **47**, 3566 (1993).

- 156) R. P. Feynman, *Phys. Rev.* **97**, 660 (1955).
- 157) R. C. Munoz, R. A. Holroyd, K. Itoh, K. Nakagawa, M. Nishikawa, and K. Fueki, *J. Phys. Chem.* **91**, 4639 (1987).
- 158) K. Itoh, R. A. Holroyd, and M. Nishikawa, *J. Phys. Chem. B* **102**, 3147 (1998).
- 159) K. Itoh, M. Nishikawa, and R. A. Holroyd, *J. Chem. Phys.* **105**, 5510 (1996).
- 160) P. Drude and W. Nernst, *Z. Phys. Chem.* **15**, 79 (1894).
- 161) A. Mozumder, *Chem. Phys. Lett.* **207**, 245 (1993).
- 162) A. Mozumder, *J. Phys. Chem. A* **106**, 7062 (2002).
- 163) A. O. Allen, 1976. Natl. Stand. Ref. Data Syst., Natl. Bur. Stand. 58
- 164) G. Ascarelli, *Phys. Rev. B* **40**, 1871 (1989).
- 165) G. Ascarelli, *Phys. Rev. Lett.* **66**, 1906 (1991).
- 166) R. C. Munoz and R. A. Holroyd, *Chem. Phys. Lett.* **37**, 250 (1987).
- 167) R. C. Munoz and G. Ascarelli, *Phys. Rev. Lett.* **51**, 215 (1983).
- 168) K. Itoh, R. C. Munoz, and R. A. Holroyd, *J. Chem. Phys.* **90**, 1128 (1989).
- 169) E. Shibamura, T. Takahashi, S. Kubota, and T. Doke, *Phys. Rev. A* **20**, 2547 (1979).
- 170) J. K. Baird, *J. Chem. Phys.* **79**, 316 (1983).
- 171) U. Sowada and R. A. Holroyd, *J. Chem. Phys.* **70**, 3586 (1979).

- 172) R. Reininger, I. T. Steinberger, S. Bernstorff, V. Saile, and P. Laporte, *Chem. Phys.* **86**, 189 (1984).
- 173) M. Reshotko, U. Asaf, G. Ascarelli, R. Reininger, G. Reinfeld, and I. T. Steinberger, *Phys. Rev. B* **43**, 14174 (1991).
- 174) E. Wigner and F. Seitz, *Phys. Rev.* **43**, 804 (1933).
- 175) C. A. M. v. d. Ende, L. Nyikos, J. M. Warman, and A. Hummel, *Radiat. Phys. Chem.* **19**, 297 (1982).
- 176) N. Gee and G. R. Freeman, *J. Chem. Phys.* **90**, 5399 (1989).
- 177) K. Itoh, R. A. Holroyd, and M. Nishikawa, *J. Phys. Chem. A* **105**, 703 (2001).
- 178) K. Itoh and R. A. Holroyd, *J. Phys. Chem.* **94**, 8850 (1990).
- 179) N. Gee, G. Ramanan, and G. R. Freeman, *Can. J. Chem.* **68**, 1527 (1990).
- 180) F. Heinrich and A. Schiltz, presented at the 6th International Conference on Positron Annihilation, Arlington, TX, 1982 (unpublished).
- 181) S. Linderoth, I. K. MacKenzie, and S. Tanigawa, *Phys. Lett. A* **107**, 409 (1985).
- 182) C. L. Wang, Y. Kobayashi, and K. Hirata, *Radiat. Phys. Chem.* **58**, 451 (2000).
- 183) M. I. Lopes, V. Chepel, V. Solovov, R. F. Marques, and A. J. P. L. Policarpo, presented at the Proceedings of the 8th Internatl. Conf. on Calorimetry in High Energy Physics, Lisbon Portugal, 1999 (unpublished).
- 184) W. J. Willis and V. Radeka, *Nuc. Inst. and Methods* **120**, 221 (1974).

- 185) S. Abachi, M. Abolins, B. S. Acharya, I. Adam, S. Ahn, and e. al, *Nucl. Inst. and Methods in Phys. Res. A* **338**, 185 (1994).
- 186) D. Schinzel, *Nuc. Inst. and Methods in Phys. Research A* **419**, 217 (1998).
- 187) J. Engler, *J. Phys. G. Nucl. Part. Phys.* **22**, 1 (1996).
- 188) M. G. Albrow, R. Apsimon, B. Aubert, C. Bacci, A. Bezaguet, and e. al, *Nucl. Inst. and Methods A* **265**, 303 (1988).
- 189) F. Arneodo, A. Badertscher, S. Baibussinov, P. Benetti, A. Borio, and e. al., *Nucl. Inst. and Methods A* **455**, 376 (2000).
- 190) E. Aprile, A. Curioni, V. Egorov, K. L. Giboni, U. Oberlack, S. Ventura, T. Doke, K. Takizawa, E. L. Chupp, and P. P. Dunphy, *Nuc. Inst. and Methods in Phys. Research A* **461**, 256 (2001).
- 191) M. I. Lopes and V. Chepel, presented at the 2002 IEEE 14th Internatl. Conf. on Dielectric Liquids, Graz, Austria, 2002 (unpublished).

## Tables

Table 8.1 – Energy Levels of Electrons at 298 K

Solvent	$V_0$ (eV)	$\Delta G_{\text{soln}}(e)$
n-Hexane	0.10	-0.33
Cyclohexane	0.01	-0.28
n-Pentane	0.01	-0.32
3-Methylpentane	0	-0.33
2-Methylbutane	-	-0.34
2,2,4-Trimethylpentane	-0.17	-0.40
2,2-Dimethylbutane	-0.26	-0.43
2,2-Dimethylpropane	-0.38	-0.44
Tetramethylsilane	-0.62	-0.62
Bis(trimethylsilyl)methane	-0.66	-0.66
Hexamethyldisiloxane	-0.70	-0.70
Data from Refs [2,33,34]		

Table 8.2 – Free Ion Yields and Mobilities at 293 – 295 K

No.	Liquid	$G_{fi}$ (electrons/100 eV)	$\mu_D$ ( $\text{cm}^2/\text{Vs}$ )
1	Tetramethylsilane	0.7	100
2	Tetramethylgermane	0.63	90
3	Neopentane	1.1	69
4	Bis-trimethylsilylmethane	0.5	63
5	Bis-trimethylsilylethane	0.41	47
6	Ethane	0.94	37
7	2,2,4,4-Tetramethylpentane	0.74	26
8	Hexamethyldisiloxane	0.30	22
9	Hexamethyldisilane	0.33	20
10	2,2-Dimethylbutane	0.58	12
11	2,2,5,5-Tetramethylhexane	0.67	12
12	2,2,4-Trimethylpentane	0.33	6.6
13	2,2,3,3-Tetramethylpentane	0.42	5.2
14	Polydimethylsiloxane	0.24	4.6
15	Propane	0.19	2.6
16	Cyclopentane	0.16	1.1
17	2-Methylbutane	0.17	0.93
18	3,3-Diethylpentane	0.23	0.76
19	2-Methylpentane	0.15	0.29
20	Cyclohexane	0.15	0.24
21	3-Methylpentane	0.15	0.20
22	n-Pentane	0.15	0.14
23	n-Hexane	0.13	0.074

24 Benzene	0.054	0.13
25 Toluene	0.051	0.08
26 Methylcyclohexane	0.12	0.068
Data from refs[2,15-19,143]		

**Table 8.3 – Ionization Detectors**

<u>Name</u>	<u>Liquid</u>	<u>Location</u>	<u>Type</u>	<u>Detects</u>	<u>Year</u>
D0	42,000 Liters Ar	Fermilab	EM Sampling Calorimeter	Electrons	1991
Walic	1 TMP	UA1 - CERN	EM Sampling Calorimeter		1988
--	210 liter TMS	Karlsruhe	Calorimeter	Cosmic Rays	1994
KEDR	24 Ton Kr	CERN	EM Calorimeter		1996
ICARUS	600 Ton Ar	Gran Sasso Italy	Time Projection Chamber	neutrinos p decay	2001
ATLAS	140 ton Ar	CERN	EM & Hadron Calorimeters	Higgs boson	2007
LXeGRIT	7 liter Xe	Balloon	Compton Telescope	gamma rays	1999
DAMA/Xe-2	2 liter Xe	Gran Sasso	Scintillator	WIMPS	1998

## **Figure Captions**

### **Figure 8.1**

Log-log plot of free ion yield versus electron mobility in nonpolar liquids. Data from refs[2,15-19]

### **Figure 8.2**

Free ion yields for n-hexane, 2,2,4-trimethylpentane and 2,2,4,4-tetramethylpentane as a function of x-ray energy. Points are experimental.[23-25] Dashed lines are theoretical.[26]; dotted line is theory. [27] Reproduced by permission.[28]

### **Figure 8.3**

Energy of the quasi-free state in rare gas fluids as a function of density. Solid lines represent recent results obtained by field ionization for Ar, [61] Kr and Xe.(see Eq. 6)[63] Recent theoretical calculations are shown for Ar by the dashed lines Ref. [64] and for Ar, Kr and Xe by the dotted lines. [65]

### **Figure 8.4**

Absorption spectra of solvated electrons in alkanes versus wavelength. Solid line is for methylcyclohexane at 295 K.[78] Dashed line is for 3-methyloctane at 127 K.[79] Dash-dot line for 3-methylpentane at 77 K.[80] Spectra have been normalized to unity at the peaks.

### **Figure 8.5**

Free energies for attachment to solutes: MeSt – methylstyrene, Sty – styrene, Bph – biphenyl, CO<sub>2</sub>, Pyr – pyrimidine, Tph – triphenylene, Dfb – *p*-difluorobenzene, Tol –toluene, But – 1,3-butadiene, Pyz – pyrazine in TMS, 2,2,4-trimethylpentane and n-hexane at 298 K and in supercritical ethane at 310 K. Data from refs. [91-93] [90,94-99]

### Figure 8.6

Rate constants for electron attachment to solutes in cyclohexane at 295 K. Solute are: 1 - CCl<sub>4</sub>, 2 - *p*-dinitrobenzene, 3 - benzoquinone, 4 - *o*-dinitrobenzene, 5 - nitrobenzene, 6 - O<sub>2</sub>, 7 - perfluoromethylcyclohexane, 8 - pyrene, 9 - anthracene, 10 - biphenyl, 11 - naphthalene, 12 - CO<sub>2</sub>, 13 - *p*-difluorobenzene, 14 - ethylbromide. Dotted line indicates calculated diffusion rate. References for rate data. [19,108-111] References for electron affinities [112-115]

### Figure 8.7

Rate constants for electron attachment to solutes in 2,2,4-trimethylpentane at 295 K. For solutes numbered 1 - 14 see legend to Figure 8.6. Other solutes: 15 - C<sub>60</sub>, 16 - SF<sub>6</sub>, 17 - C<sub>6</sub>F<sub>6</sub>, 18 - W(CO)<sub>6</sub>, 19 - Cr(CO)<sub>6</sub>, 20 - perylene, 21 - Mo(CO)<sub>6</sub>, 22 - *t*-stilbene, 23 - benzperylene, 24 - coronene, 25 - pyrazine, 26 - pyrimidine, 27 - styrene, 28 -  $\alpha$ -methylstyrene. Dotted line is calculated diffusion rate. References for rate data. [19,58,108,109,122-124] References for electron affinities. [112-115]

### Figure 8.8

Rate constants for electron attachment to solutes in tetramethylsilane at 295 K. For solutes numbered 1-28 see legends for Figs 8.6 and 8.7. Other solutes: 29 - duroquinone, 30 - CH<sub>3</sub>I, 31 - cycloC<sub>4</sub>F<sub>4</sub>, 32 - C<sub>2</sub>HCl<sub>3</sub>, 33 - phenanthrene. Dotted line is calculated diffusion rate. References for rate data. [18,19,58,90,93,122,123,125,126] References for electron affinities. [112-115]

### Figure 8.9

Rate constants for electron attachment to CO<sub>2</sub> versus the free energy of reaction in different fluids:  $\diamond$  2,2,4-trimethylpentane,[126]  $\bullet$  2,2-dimethylbutane,[139]  $\circ$  TMS,[126]  $\blacksquare$  supercritical ethane.[99]

### Figure 8.10

Drift Mobility in argon as a function of density. ● Experimental results at 55 bar.[145] — Calculation – Basak-Cohen modified (see text). --- Calculation by Hsu and Chandler.[146]

### Figure 8.11

Relative Drift Mobility as a Function of Pressure for Low Mobility Liquids. Mobility at 1 bar in parenthesis. ○ 1-pentene (0.048);[158] □ n-hexane (0.071);[19,150]◇ 3-methylpentane (0.22);[2,157] △ cyclopentane (1.02);[157] ▼ cyclohexene (1.39);[158] ◆ m-xylene (0.08);[159] ● o-xylene (0.019).[159]

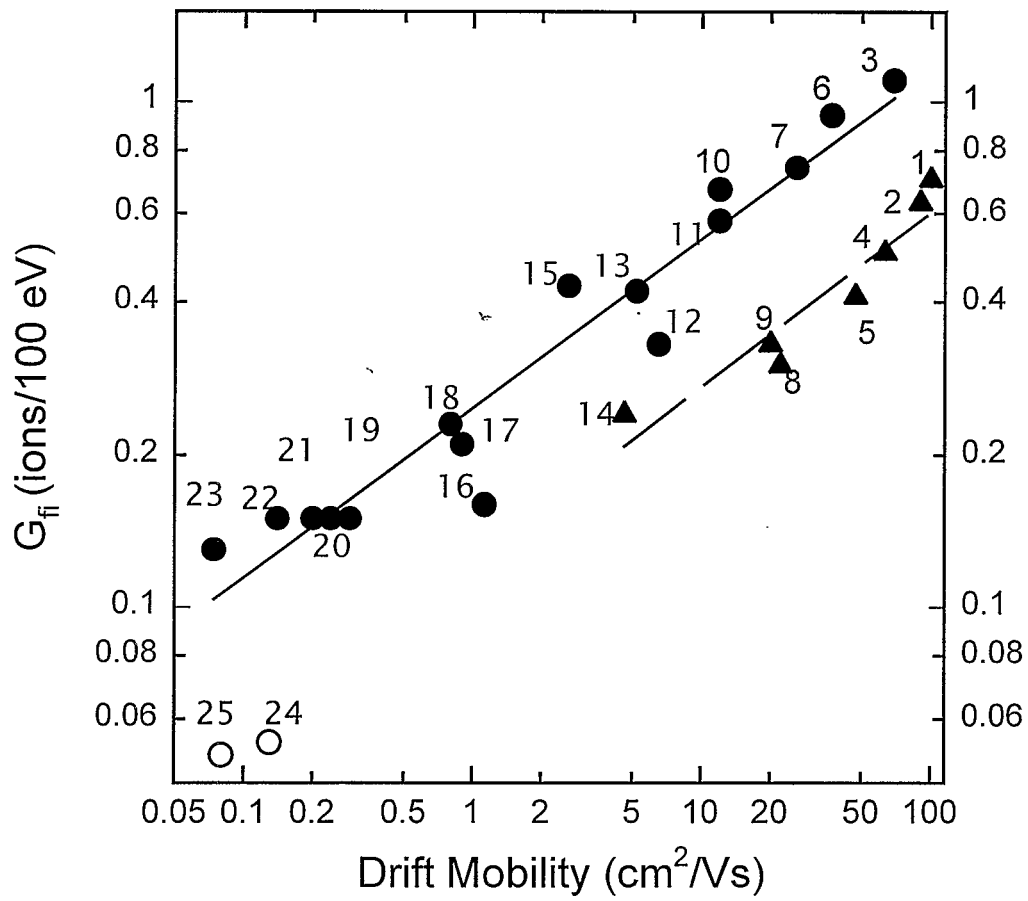


Figure 8.1

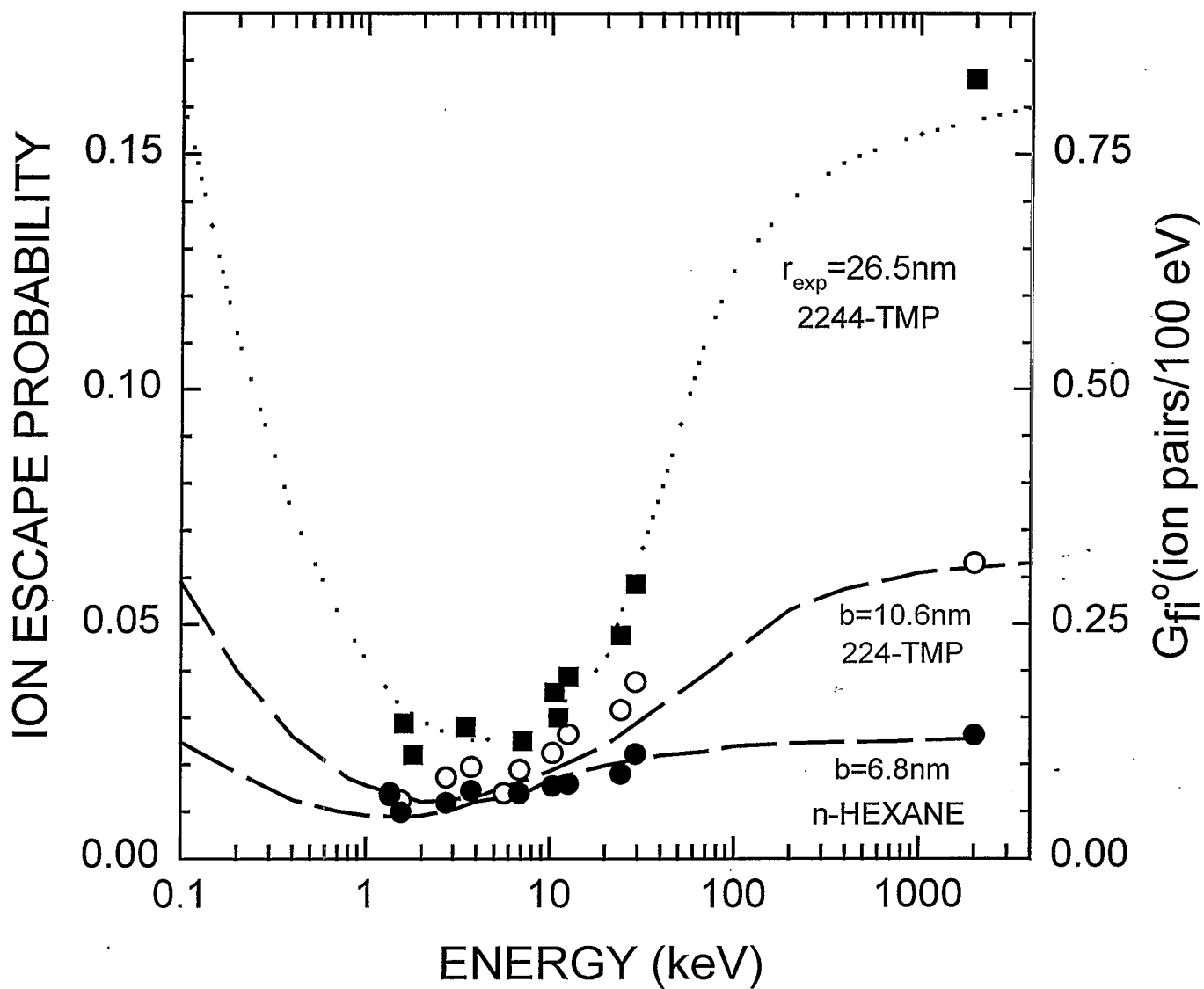


FIGURE 8.2

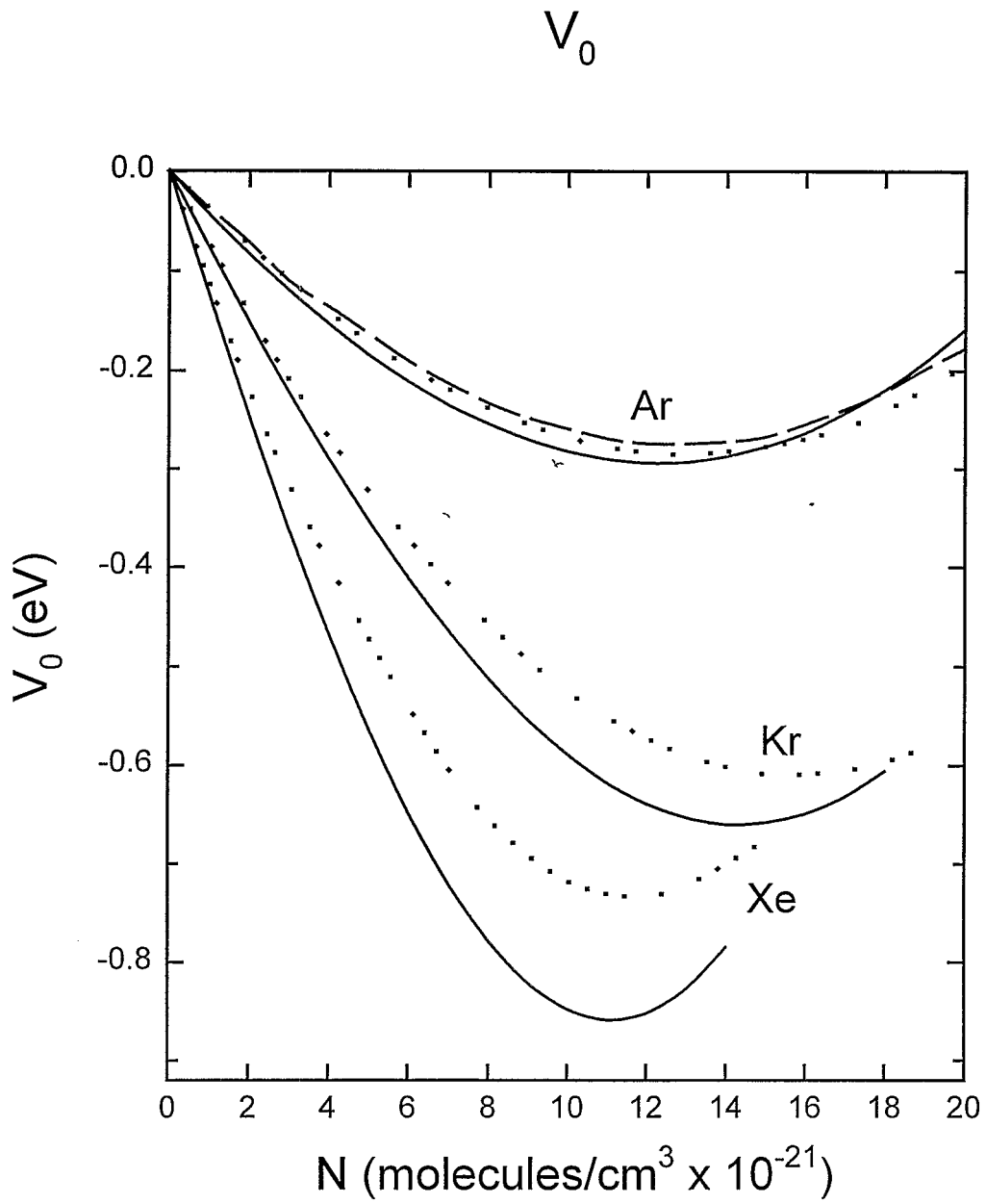


Figure 8.3

$e_{sol}^-$

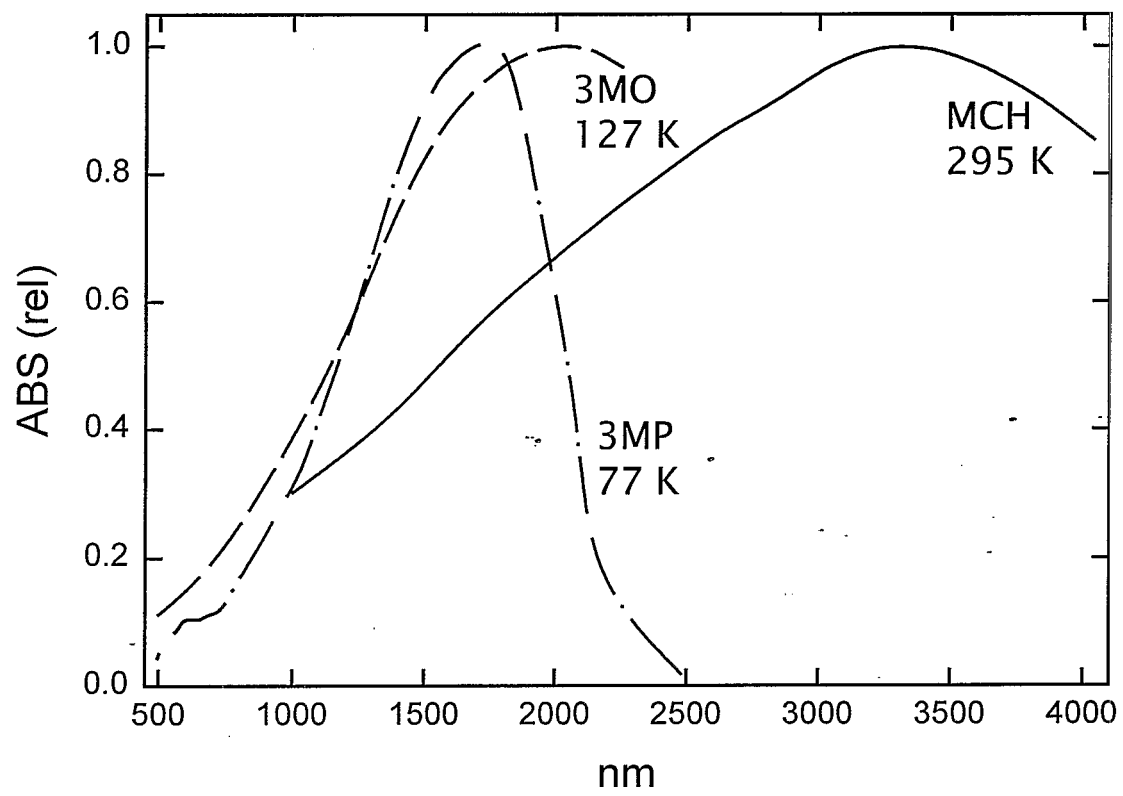


Figure 8.4

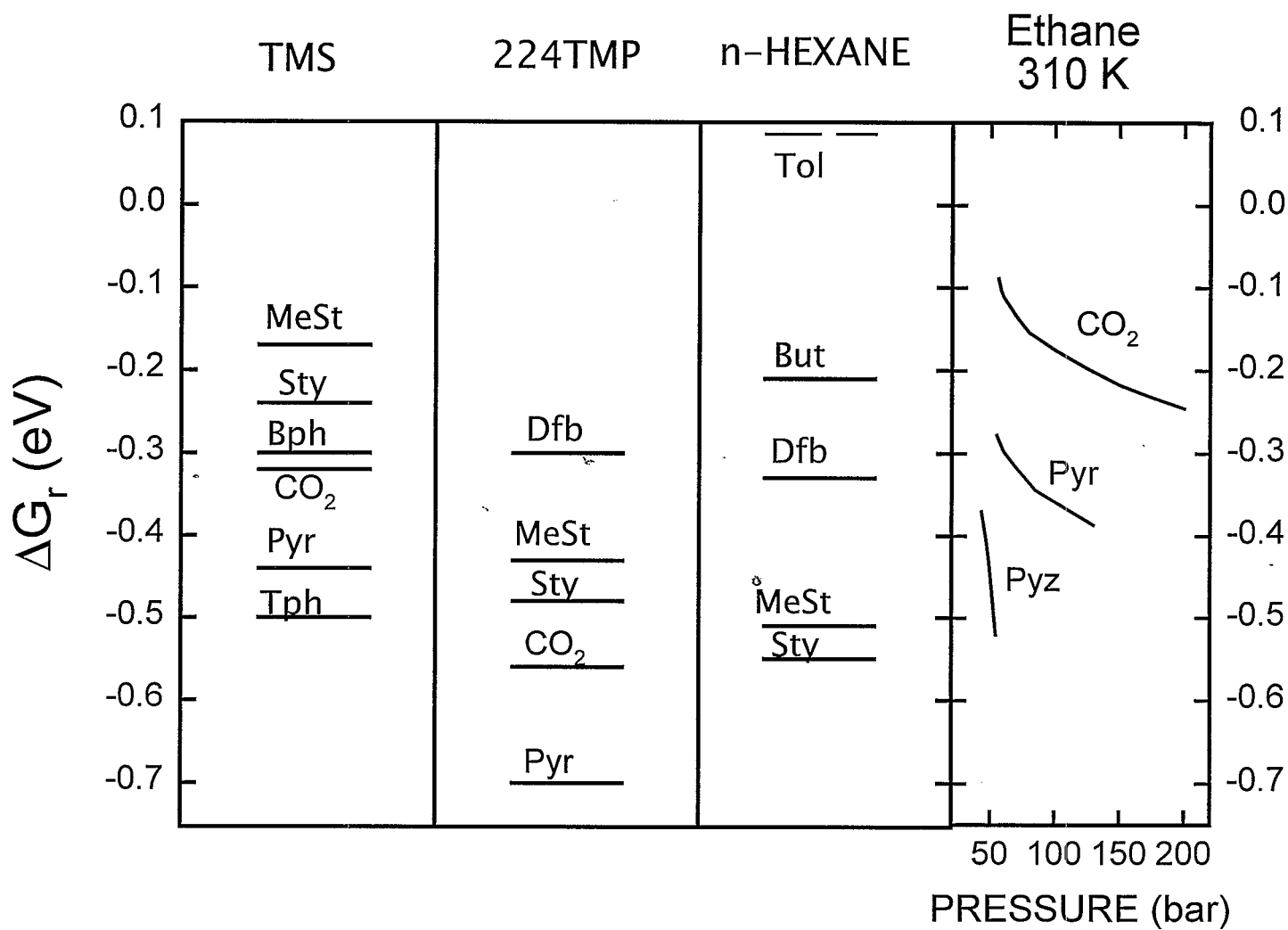


Figure 8.5

# CYCLOHEXANE

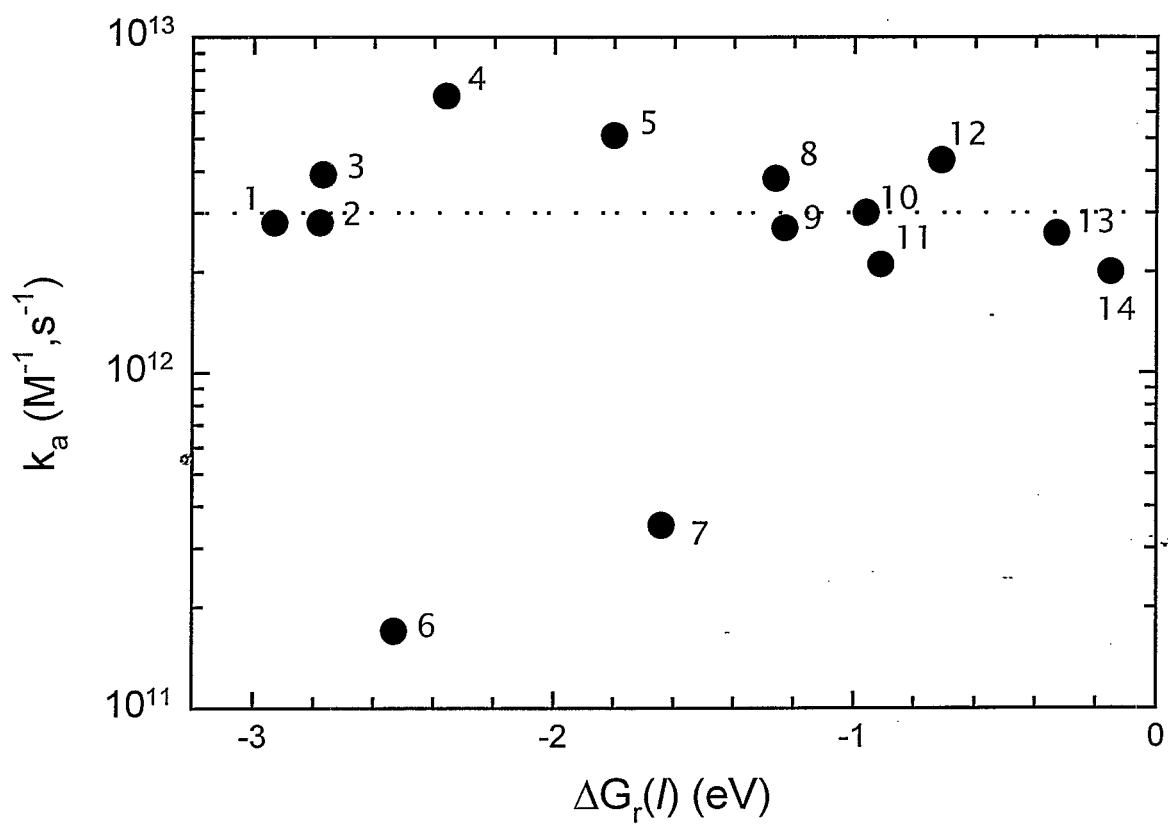


Figure 8.6

## 2,2,4-TRIMETHYLPENTANE

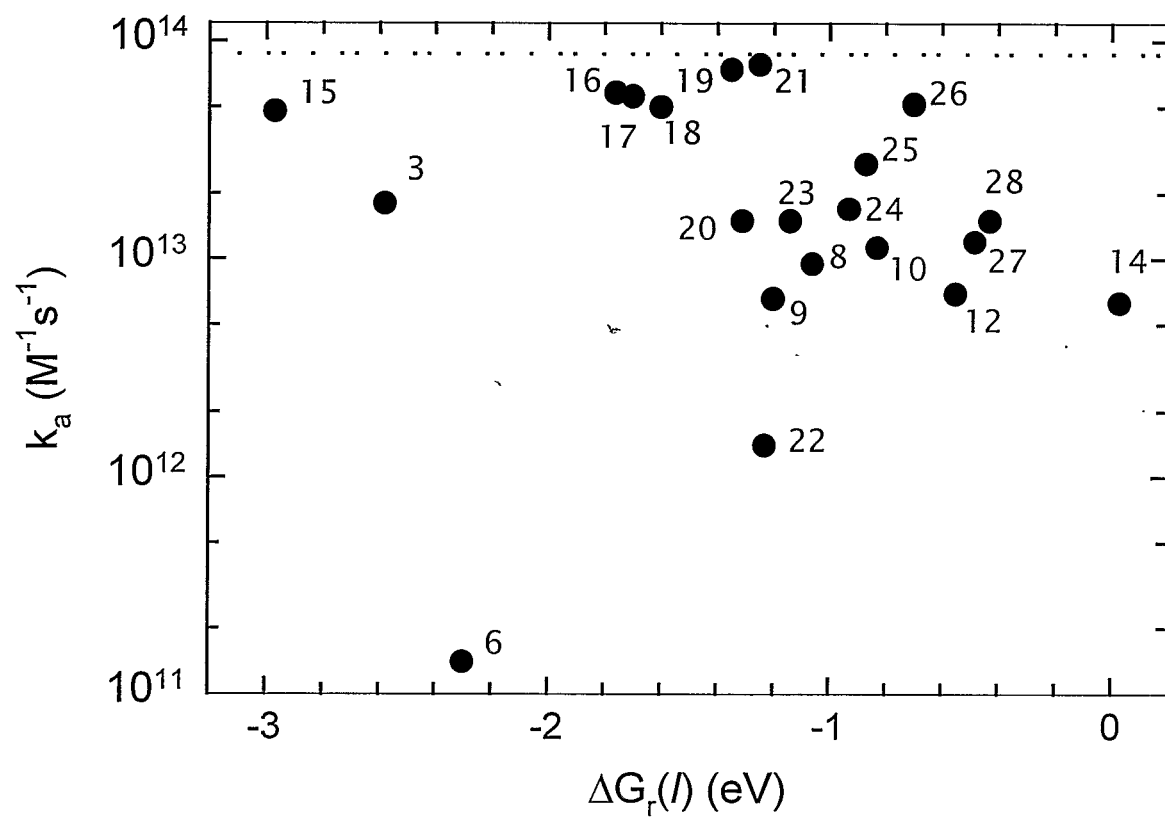


Figure 8.7

# TETRAMETHYLSILANE

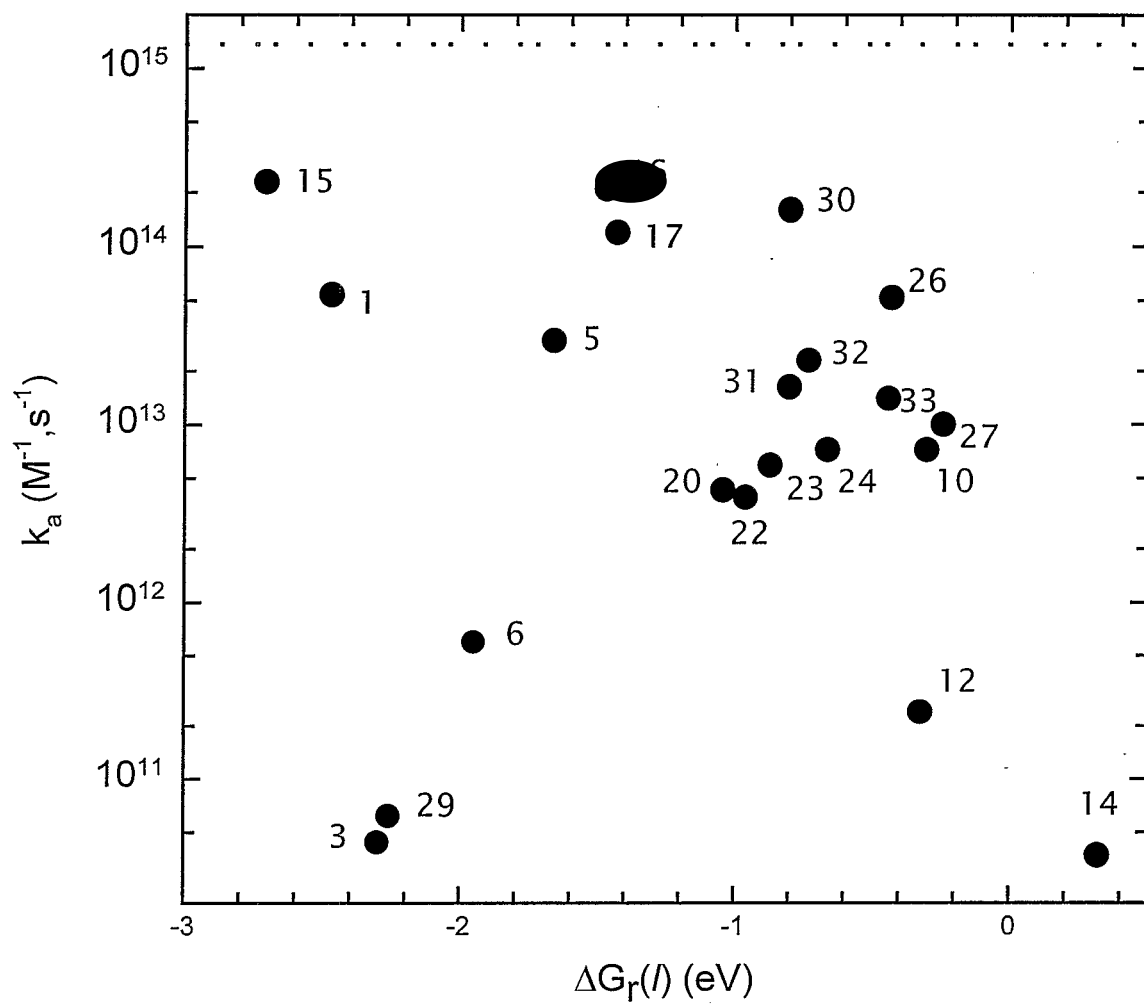


Figure 8.8

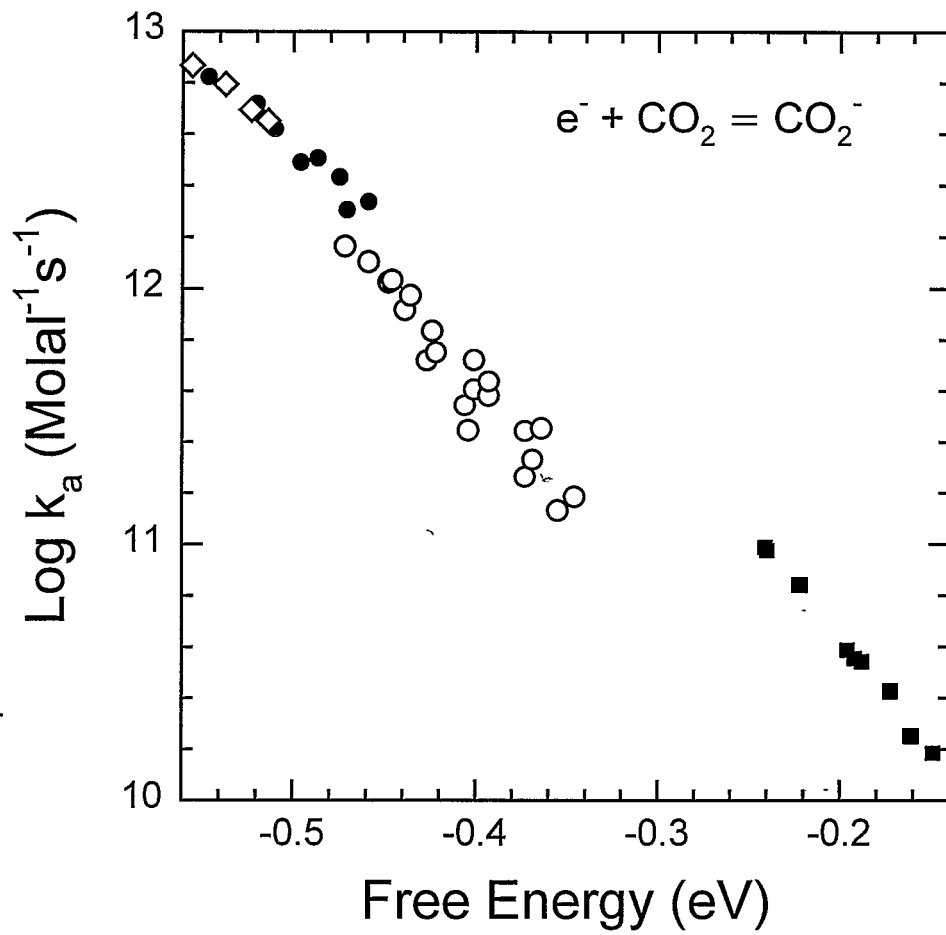


Figure 8.9

# ARGON

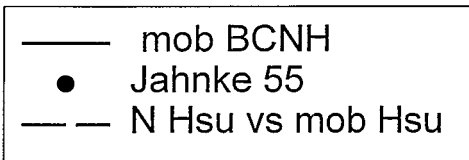
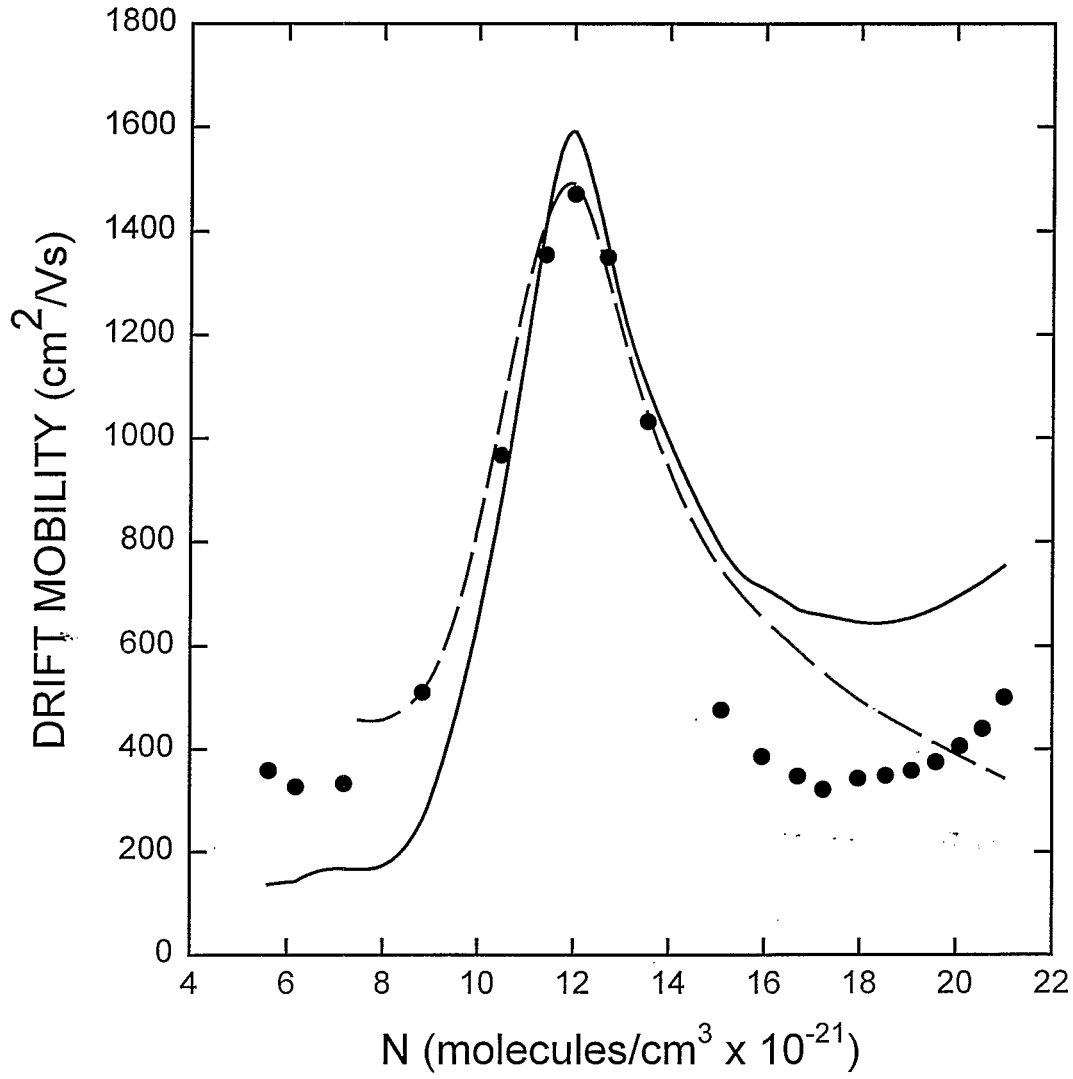


Figure 8.10

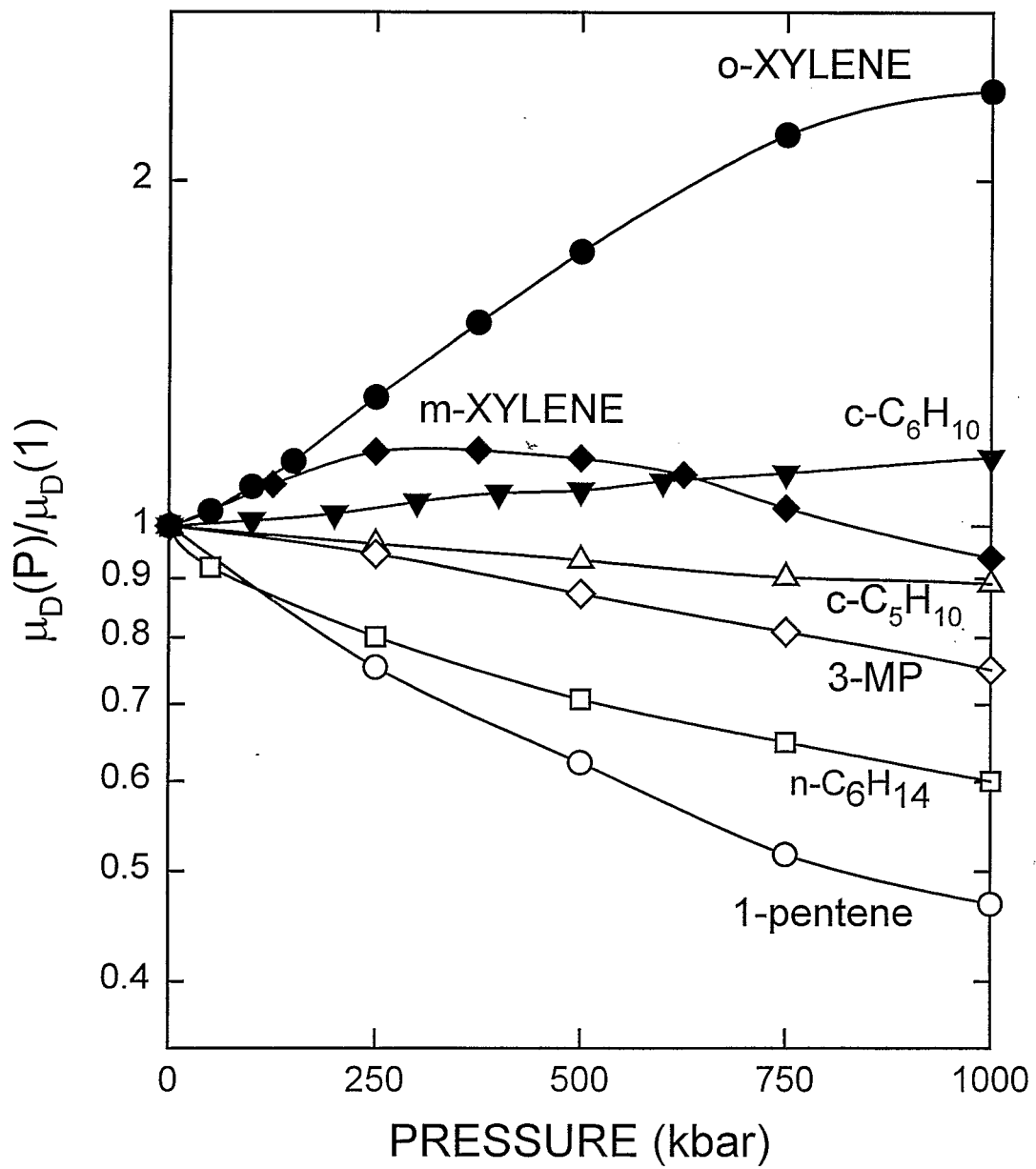


Figure 8.11